Double-Difference Earthquake Relocation of Charlevoix Seismicity, Eastern Canada and Implication for Regional Geological Structures

Meng Pang

Department of Earth and Planetary Sciences

McGill University, Montreal

Submitted:
Aug 15th, 2014

A thesis submitted to McGill University in partial fulfillment
of the requirements of the degree of Master of Science

ACKNOWLEDGEMENTS

First of all, I wish to give my earnest thanks to my supervisor Yajing Liu who has provided me with a most inspiring research environment and has guided me with the utmost patience by her rich knowledge and experiences, invaluable suggestions and firm support. Thanks for her valuable suggestions and all the effort she put into my thesis, I cannot have this achievement without her help.

I would also like to thank several individuals for assistance and warmly encouragement during my thesis. Thanks for Maurice Lamontagne, Xiuying Jin and Tim Côté who provided waveform and catalog data of Charlevoix zone for this thesis. Many thanks for Duo Li, Hongyu Yu and my boyfriend Shan Huang who provided invaluable suggestions on programming and data editing. Thanks also to Claire Lix, who helped me to translate the abstract into French.

I would like to express my gratitude to all the faculty members in the Department of Earth & Planetary Sciences, who have helped me firmly through various hard times.

Thanks to all of my friends, thank you for making my life in Montreal colorful and memorable.

Finally, thanks for my family, I owe all my success to you.

ABSTRACT

Eastern Canada is located within the North American Plate and, therefore, should have a relatively low rate of earthquake activity compared with interplate boundary. However, large earthquakes do occur in the region, especially in the Charlevoix Seismic Zone (CSZ) located about 100km downstream from Quebec City. In history, the Charlevoix Seismic Zone has been subject to five earthquakes with magnitude 6 or larger ($M \sim 7$ in 1663; $M \sim 6$ in 1791 and 1860; $M \sim 6.5$ in 1870; $Ms \sim 6.2 \pm 0.3$ in 1925). However, the regional geological structures of the CSZ are not well understood. As one of the most seismically active region in Eastern Canada, the earthquakes in the CSZ are a significant hazard. Therefore, improved knowledge of distribution and seismic characteristics of these events provides a great benefit for understanding the seismic hazard of the CSZ. In this thesis, I apply earthquake location technique on discovering fault features in CSZ.

Earthquake location, as a basic technique in seismometry, plays an important role in the studying of fault structures. The double-difference earthquake location algorithm (HYPODD) is able to get high-resolution hypocenter locations by introducing the residual between observed and calculated travel times between two events and removing the effects of the un-modeled velocity structure. In this thesis, the resolution of double-difference location algorithm was analyzed using the seismic data of Canadian National Seismograph Network(CNSN) from Jan,1988 to Oct, 2010. The double-difference earthquake location algorithm was used to relocate more than 2000 earthquakes in the Charlevoix seismic zone (CSZ), using a layered velocity model. The location results of initial catalog data and double-difference relocation results visually compare with each other, and the cross section of the northeast part in CSZ shows two nearly parallel faults dipping about 60 degree to the southeast. This provides evidence that there are minor rifting geological features underneath the St-Laurence River.

Key Words: Earthquake Location; Double-difference Earthquake Location; Charlevoix Seismic Zone

RÉSUMÉ

L'Est du Canada est situé au cœur de la plaque nord-américaine et, par conséquent, devrait avoir un taux d'activité sismique relativement faible. Cependant, de grands séismes se produisent dans la région, particulièrement dans la Zone Sismique de Charlevoix (ZSC), située à environ 100 km en aval de la ville de Québec. Dans le passé, la Zone Sismique de Charlevoix a fait l'objet de cinq séismes avec une magnitude de 6 ou plus ($M \sim 7$ en 1663; $M \sim 6$ en 1791 et 1860; $M \sim 6.5$ en 1870, $Ms \sim 6.2 \pm 0.3$ en 1925). Les structures géologiques régionales de la ZSC ne sont cependant pas bien comprises. Étant la région sismique la plus active de l'Est du Canada, la ZSC peut causer un risque sociétal important. Par conséquent, une meilleure connaissance de la distribution et des caractéristiques sismiques de ces événements améliorerait la compréhension des risques sismiques de la Zone Sismique de Charlevoix.

La localisation des séismes, technique de base en seismométrie, joue un rôle important dans l'étude des failles actives. L'algorithme de localisation des séismes par double différence (HYPODD) permet d'obtenir en haute résolution la localisation de l'hypocentre, en introduisant le résiduel entre la différence de temps de trajet observée et calculée de deux événements, et en supprimant les effets de la vitesse de la structure non modélisée. Dans cette thèse, la résolution de l'algorithme de localisation des séismes par diffrence double a été analysée en utilisant les données sismiques de la Commission Géologique du Canada de 1988 à 2010. Cet algorithme a été utilisé pour relocaliser plus de 2000 séismes dans la zone sismique de Charlevoix (ZSC), en utilisant un modèle de vitesse relative d'une étude précédente. Les résultats de localisation de données de catalogue initial et les résultats de localisation par double différence sont comparables. La coupe de la partie nord-est de la ZSC montre un plongement de faille d'environ 60 degrés vers le sud-est et met en évidence la présence de caractéristiques géologiques mineures de failles de rift sous le fleuve Saint-Laurence. Ceci est un progrès dans l'identification de l'orientation de la faille et permet de mieux comprendre la microtectonique de la CSZ.

TABLE OF CONTENTS

LIST OF TABLES

LIST OF FIGURES

Figure page

CHAPTER 1
INTRODUCTION

1.1 Introduction

In the earth sciences, a very important yet unanswered question is why there are some distinct seismic zones in stable continental regions (**SCR**). **SCR** are different from active plate boundaries where earthquakes occur frequently. The study of **SCR** seismic zones is important due to the significant hazard they pose to populated regions in vicinity. Scientists have recognized that most of **SCR** seismic zones are caused in rifted portions of the crust. However, it remains unclear why some portions of these ancients rifts are seismically active while others are not.

The Charlevoix Seismic Zone (CSZ) is located 100km northeast of Quebec City in Easten Canada, which is part of the stable continental region of the North America plate. Historically, five earthquakes with magnitudes equal to or exceeding 6.0 Mw have occurred here and approximately 200 earthquakes are recorded by the Canadian National Seismograph Network annually. Regional seismicity studies in the CSZ are integral in the investigation of the relationship between the tectonic structure of the seismogenic basement and current earthquake activity, and used to evaluate the seismic risk within this area. From previous studies, we know the CSZ earthquake hypocenters are located in the Precambrian basement rocks, which have been affected by several tectonic events including Grenvillian collision ($\sim 1100 - 900 Ma$), Iapetan Ocean rifting ($\sim 700Ma$) and closure ($\sim 450Ma$), and meteorite impact ($\sim 350Ma$). Numerous hypothese have been proposed to explain the distribution of earthquakes in the CSZ, such as weakened crust and amplified stress differences cause by the meteorite impact ([19], [18]), stress modified in the process of glacial rebound ([13], [26], [25]), and high pore fluid pressure or low coefficent of friction at the focal depths ([17]). While, more than 20 years of seismic observation by the Charlevoix Local Telemetered Network (CLTN) has shown that hypocenters do not concentate on planar structures, although the microtectonic structures are still not clear. Accurate earthquake hypocenter locations could provide information identifying potential seismogenic features.

Earthquakes in the CSZ make a significant contribution to the natural hazard risk in eastern Canada, due to their proximity to major population centers, e.g., Montreal and Quebec City ([1])(Figure 1–1). Understanding the earthquake source parameters and mechanisms involved in the occurrence of these earthquakes will benefit earthquake hazard analysis in eastern Canada. The study of hypocenters in the CSZ has found that most large faults seem to bound active volumes instead of being active themselves ([16]). Seismic activity in the central impact zone is frequent with smaller magnitude events, in contrast, larger and more infrequent earthquakes occur on the CSZ paleorift faults.

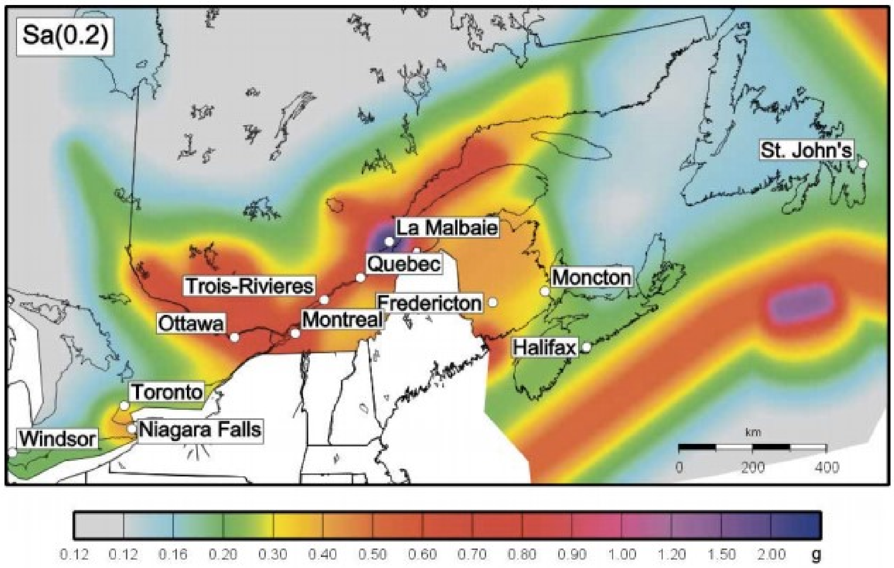

Figure 1–1: Map of southeastern and southwestern Canada showing spectral acceleration(Sa)(0.2) hazard (median values of 5% damped spectral acceleration for a probability of 2%/50 years) and the locations of most cities for which deaggregation is performed. The high hazard value of La Malbaie and Quebec City dominated by Charlevoix earthquakes at close distances. ([11])

Understanding the cause of intra-plate earthquakes in the CSZ is really a very difficult problem, due to undetermined complicated minor features in its seismogenic faults. In this study, I use the small magnitude(magnitude larger than 2.0) earthquake data (Jan. 1988-Oct. 2010) primarily from the local network monitoring to examine the minor fault features and its orientation by using the double-difference location algorithm (program short for HYPODD) developed by Waldhauser and

Ellsworth ([24]). HYPODD can greatly reduce the errors in relative earthquake locations introduced by uncertain velocity models, by fulfilling a set of conditions for taking advantages of double difference algorithm.

In summary, the purpose of my master research project is to relocate earthquake hypocenters in the Charlevoix seismic zone. My main work focuses on the hypocenter clusters, which provide information about the orientations of the regional seismogenic faults. The seismic knowledge of the locations and orientations of the brittle faults of the CSZ in the Precambrian Basement rocks will help us look into and understand the long and complex tectonic processes of the Appalachians Nappes. Also, the present seismic activity will tell us how ancient faults are being reactivated in the modern stress field.

1.2 Organization of Thesis

* Chapter 1 introduces the background, purpose and significance of my research topic as well as the layout of this thesis.
* Chapter 2 talks about the geological setting and regional historical seismicity of the study area.
* Chapter 3 provides the data set and methods used to do the earthquake relocations in CSZ and also presents a brief review of the workflow and parameters used in HYPODD software packages.

* Chapter 4 shows the results of relocation applying double-difference algorithm to the study area, including origin locations, catalog relocations, waveform relocations and focal depths.
* Chapter 5 is a discussion on the conclusions of the relocation results with a comparison to tectonic features of Charlevoix zone.
* Chapter 6 summarizes the findings of the research and makes recommendations for future research in CSZ.

CHAPTER 2
GEOLOGICAL SETTING AND SEISMICITY OF THE STUDY AREA

2.1 Introduction

The Charlevoix Seismic Zone (CSZ) is located less than 125 km east from Quebec City in the St. Lawrence valley of Quebec, as the most seismically active region in eastern Canada. In history, it has been the site of five moment magnitude $M > 6$ earthquakes since 1663 ([3], [4])) as well as continuous 200 earthquakes every year. Like most intraplate earthquake zones, the cause of the focus of seismic activity is not well understood.

In general, intraplate seismicity is associated with preexisting weak structures such as ancient rift zones, while such intense seismic activities in small areas are often attributed to local effects. After a long-term debate on the relative importance of the two potential sources of weakness: the CambroOrdovician St. Lawrence rift, which strikes NE SW along the river; and the Charlevoix Impact structure (Figure 2–1), among the largest ($\sim$ 54 km in diameter) ([22]), and the most accessible meteorite impact structure in eastern North America, Adams and Basham ([2]) attributed the earthquakes in CSZ to the reactions of regional weakened rift faults caused by the crater. They proposed that the impact structure is the key of making the crust weaken to yield more easily to postglacial strain. This structure, which is at the heart of the Charlevoix Seismic Zone, overprints Iapetus rift faults and the Logans

Line marking the edge of the Appalachian Orogen. The Charlevoix Seismic Zone is the locus of the highest seismic hazard in continental eastern Canada.

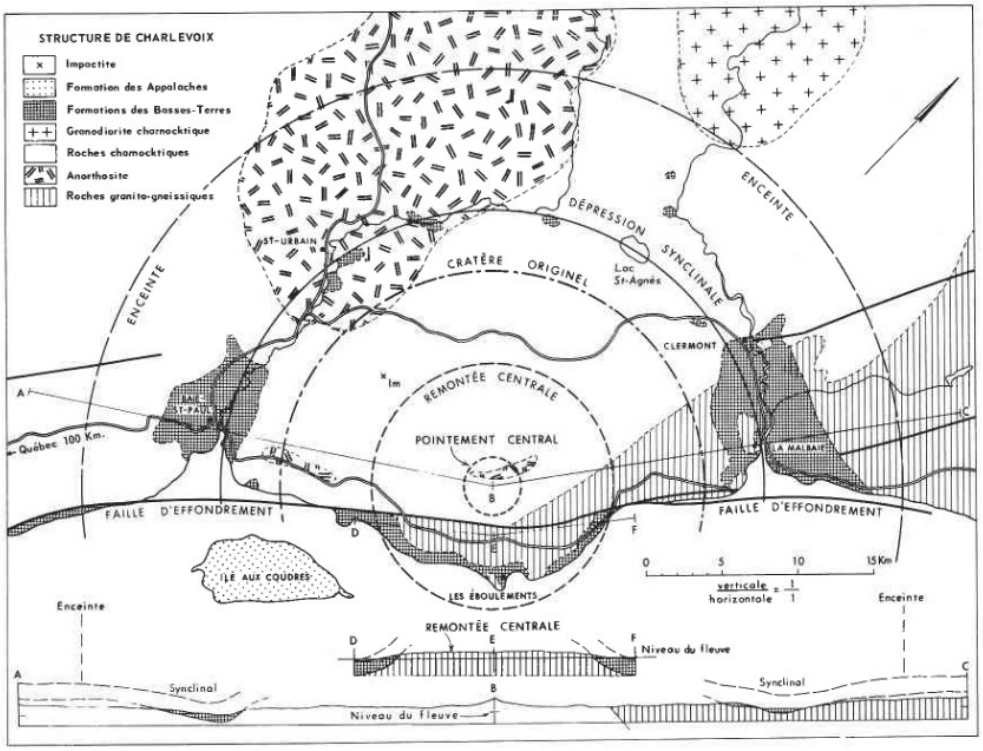

Figure 2–1: Charlevoix structure. Map and schematic cross section showing location of impactite. Im 1, outcrop; Im 2, sub-outcrops. In the section, the broken line represents the original crater without its ejecta. the Heavy lines beneath the cover of Ordovician limestone represent hypothetical stratigraphic horizons in the Precambrian. Slide-surfaces are shown by continuous lines. The v pattern represents the zone of maximum development of shatter cones, and the vertical shading shows the zone of maximum shock metamorphism. Charlevoix geological structure affects the Canadian shield and its Paleozoic cover, the rift zone along the St. Lawrence, and the overthrust Appalachian rocks of Ile aux Coudres ([8]))

The Charlevoix impact structure gives the region its singular landscape. The peripheral ring trough, $\sim$ 20 km in radius, forms a prominent open valley that locally reaches an altitude of 250 m. The highest point in the valley is nearly 850 meters below the mean elevation, approximately 1100 m, of the external Laurenceian plateau and 550 m below the central uplift, Mont-des- boulements, which stands 780 m above sea level. The overall morphology of the Charlevoix impact structure matches that of a complex impact crater ([22]). Shatter cones, mylolisthenite injections and shock-related planar deformation microstructures in quartz and feldspar are widespread, hence providing compelling evidence for the extent of shock metamorphrism. The age of the impact is poorly constrained. Recently acquired Ar-Ar data from impact melt rock and pseudotachylite give a late-Ordovician age which appears to be in better agreement with field relationships than the previously reported K-Ar Devonian-age.

Based on historical large earthquakes and current frequent earthquake rates, the Charlevoix Seismic Zone is the zone stands for its high seismic hazard. Since the arrivals of the first Europeans in the early 1600s, it has been subject to five earthquakes of magnitude 6 or larger. While much has been published describing the seismicity in the CSZ, double-difference relocation method has not been applied to explain the geological structures behind the partitioning of seismicity. Kim et al (2000) have shown that double-difference relocation results can show geological structures and Lamontagne ([16]) has revealed that much of the earthquakes are not occurring along planar structures. In contrast, quite a lot of events appear to be located in fractured volumes of rock bounded by the major rift faults by improvements in hypocenter location and analysis of microseismicity focal mechanisms in the 1990s. Therefore, both the impact structure and the rift faults appear to play a key role in the distribution of seismicity in the Charlevoix Seismic Zone.

2.2 Geologic Setting

The Charlevoix region displays a rich geological heritage by a series of tectonic events spanning the last 1.1 billion years. It is located at the present-day erosional limit of three geological landmarks in central and eastern North America. Precambrian charnockitic gneisses overlain by Ordovician sedimentary rocks form the basement. An elongated outside border of Cambro-Ordovician sediments of the St. Lawrence Platform interposes between the Mesoproterozoix crystalline rocks of the Grenville Province of southeastern Laurenceia and the thrust-accreted rocks of the Appalachian Orogen. In other words, the Charlevoix region lies along the late-Neoproterozoic to Cambrian St. Lawrence rift system, inboard from the Appalachian front with thrust activity (400Ma) over the Precambian and to Upper Ordovician rocks along a plane dipping 20 degree towards the SE. Orogeny-driven faulting and fault reactivation likely occurred through the Paleozoic and Mesozoic ([12]).

In fact, given the turbulent geological history of the Charlevoix region, crosscutting and overprinting structural and tectonic relationships in the area are in places difficult to decipher, and their full significance is somewhat debatable. One of the possible tectonic series statements: the rocks made up the core of 1100 990 Ma

Grenville orogeny, which resulted from a series of exotic terranes accreting onto the southeast margin of Laurenceia, now form the basement of the Charlevoix area. From late Proterozoic to early Paleozoic, the Rodinia supercontinent started to breakup and the Iapetan Ocean formed resulting in the rifting event ([14]). The St. Lawrence paleorift system was thus formed by a series of normal faults. After the closing of the Iapetan Ocean, the Appalachian Nappes formed and were thrust over the North American continent as far west as the St. Lawrence in the Charlevoix area with Logan s Line running through the CSZ.

Following this, the region was impacted about 350 Ma ago by a meteorite resulting in a large crater ([8]). While evidence for a major impact structure is conclusive, the role of Iapetus rifting and subsequent Appalachian telescoping in the development and reactivation of the fault network and in the preservation of the St. Lawrence Platform sediment fringe is likely more important than initially anticipated. Therefore, the meteorite impact event added on to an already multiplex geological history, significantly weakening the crust and making it more prone to subsequent seismic activity. The last regional significant tectonic episode was the normal sense reactivation of the Iapetan rift faults cause of the Atlantic opening in the Mesozoic ([20]).

Here I also mention that, due to the afterwards regional uplift and erosion led to over one to two kilometers of disinterment, the latter day crater-like topographic expression of the Charlevoix impact structure does not depicted directly the original crater. Thus, the latter day topographic expression is the integrative result of a series of geological properties and activities, including differential erosion between variably crushed rocks, the shattering density and erosion crumbliness being related to impact craters deep infrastructure. The impact melt-derived rocks as part of quit little remaining of the craters fill deposits have been discovered in two small outcrops 9 and 10 km northeast of the central peak and as boulders in glacial reworked [Rondot, 1971](Figure 2–2).

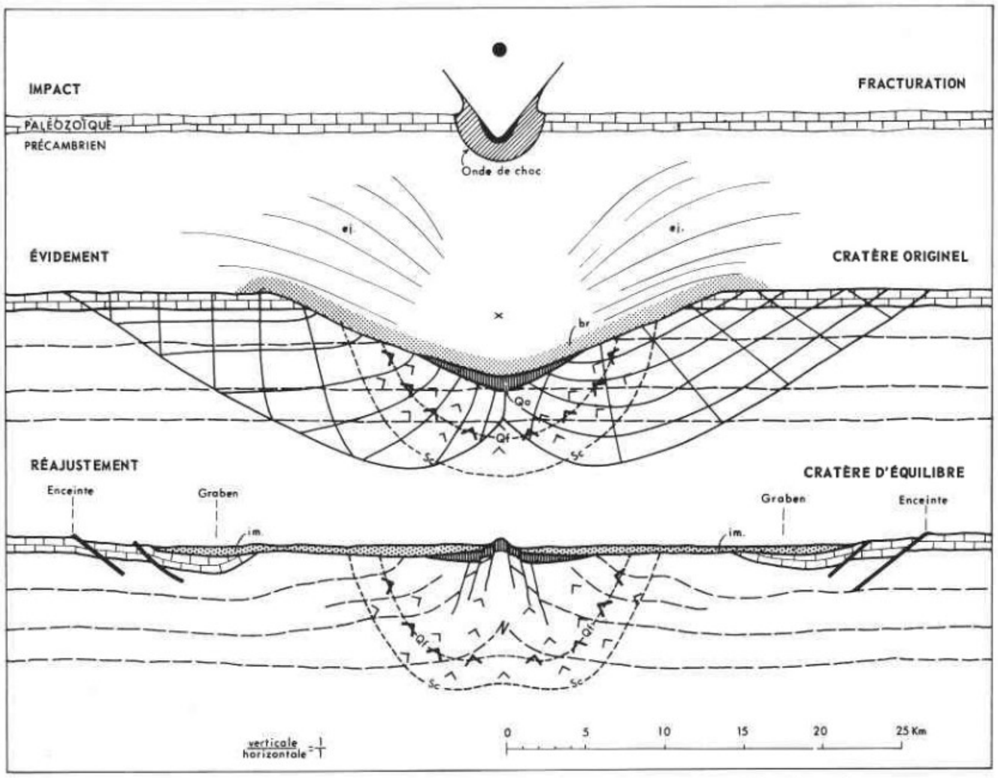

Figure 2–2: Schematic cross sections showing the progressive development of the Charlevoix complex impact structure. ([8]) (1) Geological setting of the pre-impact target region. (2) Impact/compression and excavation stage with the development of a transient crater. (3) Modification stage: paired development of the peripheral collapse and central uplift, and thinning and draping of the original melt layer over the uplifted rocks. So the final structures include the central uplift mountain area, the annual hills/rim produced by the movement of normal faults towards the interior.

2.3 Charlevoix Seismic Zone

Based on historical and current earthquake rates, the Charlevoix Seismic Zone (CSZ) is the zone with the highest seismic hazard in continental eastern Canada(Figure

2–1). Five earthquakes of magnitude 6 or larger has happened in CSZ in 1663 ($M \sim 7$); 1791($M \sim 6$); 1860($M \sim 6$); 1870($M \sim 6.5$); and 1925(MS 6.2 ± 0.3).

In the 1970s, the earthquake potential of the area led the Government of Canada to conduct two field surveys that defined its main seismotectonic characteristics ([19], [18]). Hypocentres cluster along or between the mapped Iapetan faults (also called St. Lawrence paleo-rift faults). The largest earthquake of the 20th century was the 1925 earthquake and its focal mechanism has one nodal plane consistent with a reactivation of a SE-dipping paleo-rift fault. The installation of a permanent seismograph network in 1978 has helped to define additional characteristics of the area. The St-Laurence fault, one of the major rift faults of the CSZ, was formed in the late Precambrian but was also active after the Devonian meteor impact ([10]), probably during the early stages of the opening of the Atlantic Ocean in late Triassic-Jurassic times ([20]). This fault is not particularly active but appears to bound concentrations of hypocenters ([16]). Earthquakes occurs between the surface to 30 km depth, in the Precambrian Shield, that outcrops on the north shore of the St. Lawrence River or is found beneath Logans line and the Appalachian rocks.

2.4 Past studies on CSZ

In history, the CSZ has been the focus of various geophysical studies since its high regional activity as the most active seismic regions in eastern North America ([6]). These contain the studies focus on investigations of velocity structure, including a seismic reflection-refraction survey ([6]), mircoearthquake surveys ([19],

[18], [17]), analysis of the teleseismic events [Hearty et al., 1977], receiver function analysis ([7]), shear wave splitting and anisotropy studies and focal mechanisms of microearthquakes ([15], [5]), as well as quite a few earthquake prediction studies in the late 1970s and early 1980s ([6]). From my study data, I find most of Charlevoix earthquakes occur in the depth range 5-25 km with some as deep as 30 km (Figure 2–3). However, according to seismic data of Lamontagne's doctor thesis, roughly 80 percentage of the earthquakes occur in the depth range 5-15km in Grenville basement. And based on this hypothesis, Lamontagne and Ranalli (1996) attribute earthquakes to faulting above the brittle-ductile transition to depths of at least 25 km and the reactivation of pre-existing faults could be due to high pore-fluid pressure at temperatures below the onset of ductility for hydrated feldspar at about 350 and/or a low coefficient of friction, possibly related to unhealed zones of intense fracturing. The distribution of spatially clustered earthquakes within the Charlevoix seismic zone indicates that very few earthquakes have occurred on the same fractures with similar focal mechanisms, implying that these faults zones occur in highly fractured rocks especially those within the boundaries of the Devonian impact structure ([17]). The hypocenter-velocity simultaneous inversion of local P and S wave produced a velocity model that revealed areas of high-velocity bodies at mid-crustal depths ([23]). These areas were interpreted to be stronger, more competent crust that separates CSZ earthquakes into two main bands elongated along the St. Lawrence River. CSZ focal mechanisms are quite variable in orientation and, to a lesser extent, faulting style. It is generally assumed that, on the average, most Charlevoix earthquakes occur as thrust events on pre-existing SE steeply (60°) dipping faults. Also, the larger events

concentrated outside the meteor impact at both ends of the seismic zone ([19], [16]) indicates that the region itself may have sub-areas with different rheological properties due to the pressure of the meteor crater and its faults.

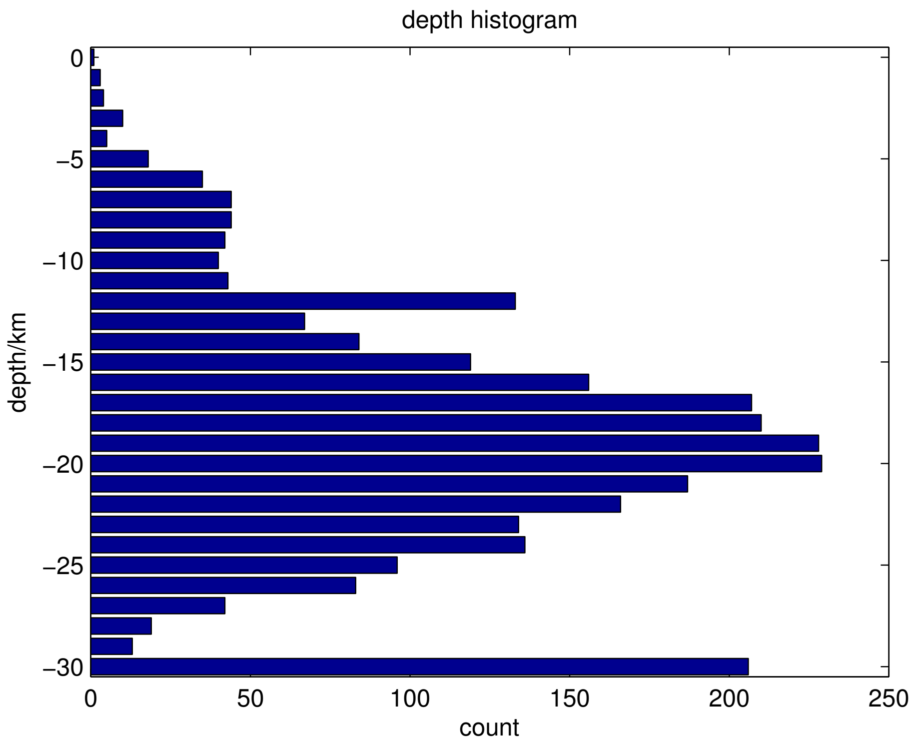

Figure 2–3: Number of earthquakes distribution with depth, in CSZ Jan, 1988-Oct. 2010, acquired from CNSN.

CHAPTER 3
EARTHQUAKE LOCATION THEORY AND METHODS

3.1 Introduction

An earthquake is the result of a sudden release of energy in the Earths crust and generates seismic waves, which propagate through a medium such as the layers of rocks and can be recorded by seismometers up to great distances. Therefore, the characteristics of seismic waves include seismic source, path of propagation, wavefield effect and instrumental effect (Figure 3–1). The instrumental effect will not be discussed here as it is just an artificial factor for improving the signal quality. The list below is the origins of the first three factors:

* seismic source: an earthquake is caused by fault slip and generates seismic waves to travel through medium. The waveform record is affected by the magnitude of energy release and rupture dynamics.
* path of propagation: the characters of the medium that seismic waves travel through, such as material density, rigidity and so on, will affect the waveform shape.
* wavefield effect: when a seismic wave propagates to the nearby area of seismic stations, it is amplified by the characters of the local region.

This chapter describes the methodology of double-differences earthquake relocation in Eastern Quebec.

3.2 Double-difference Relocation Algorithm

The epicentral location and the focal depth are critical parameters for seismic hazard assessment, seismological research, and seismotectonic study. The accuracy of hypocentre location determination depends on several factors, including the network geometry, available phases, accuracy of arrival-time, and the crustal structure (Pavlis, 1986; Gomberg et al., 1990). The accuracy of the arrival time of the phases, by itself, plays a critical role in estimating the hypocentral location. The methodology for the hypocentral location is also important. Different hypocentral locating algorithms can give slightly different results with different accuracy. As will be shown later, the HYPODD algorithm ([24]) used in this thesis proved to give stable results and to work well for local and regional earthquakes in eastern Quebec.

Double differential relocation algorithm is to make use of a number of earthquake events, which have close hypocenters and similar earthquake ray paths (as known as multiplet) (Figure 3–1), to simultaneously relocate earthquakes. The DD technique takes advantage of the fact that if the hypocentral separation between two earthquakes is small compared to the event-station distance and the scale length of velocity heterogeneity, the the ray paths between the source region and a common station are similar along almost the entire ray path. Since the characteristics of hypocenters are similar, it is thought that the focal mechanisms are substantially the same. So the ray paths between the source region and a common station are very similar (almost the same) along the entire ray path. The site effects of different events arriving at the same station are also the same, except for the difference of the hypocentral separation. This is the key concept that double-differential earthquake relocation algorithm adopts.

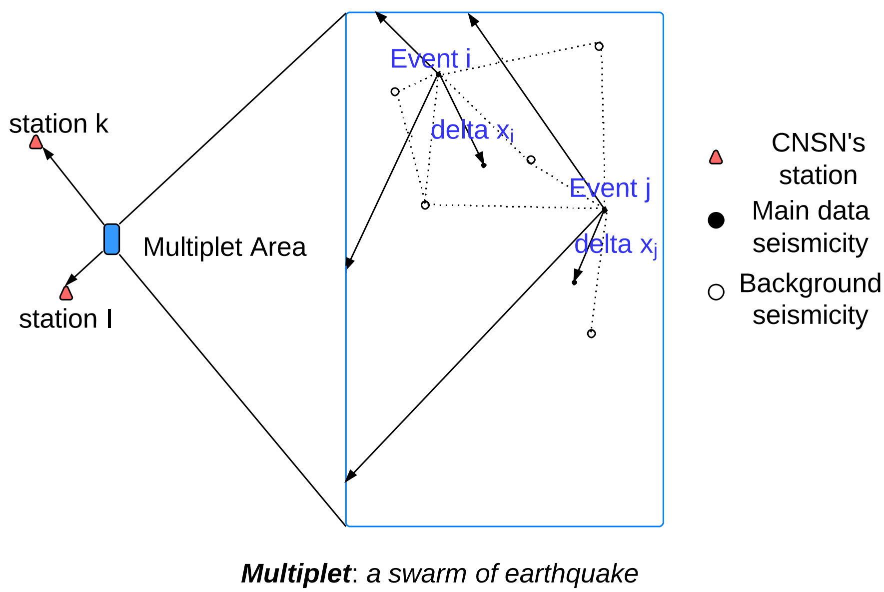

Figure 3–1: Illustration of double-difference earthquake relocation algorithm. Triangles stand for 2 stations that are close to each other and the rectangle illustrates the multiplet area where many seismic events occur.

According to ray path theory, the arrival time, T, for an earthquake, I, to a seismic station, k, is expressed as

$$T_i^k = \tau^i + \int_i^k u ds \tag{3.1}$$

where τ is the origin time; u is the slowness field that seismic waves travel through; ds is length of an element of the path. After eliminating the high order terms a truncated Taylor expansion can be obtained as follows,

$$\frac{\partial t_k^i}{\partial m} \Delta m^i = r_k^i \tag{3.2}$$

Where r_k^i is the travel-time residuals between the observed and theoretical travel time for an event i in observation k, $\Delta m^i = (\Delta x^i, \Delta y^i, \Delta z^i, \Delta \tau^i)$ is the change in hypocentral parameters $\Delta x^i, \Delta y^i, \Delta z^i, \Delta \tau^i$ for event i.

However, equation 3.2 cannot be solved directly. Fréchet (1985) came up with a method using a pair of events (i, j). After calculating the difference between equation 3.2 for a pair of events (i, j), residual between observed and calculated differential travel time between these two events is:

$$\frac{\partial t_k^{ij}}{\partial m} \Delta m^{ij} = dr_k^{ij} \tag{3.3}$$

where $\Delta m^{ij} = (\Delta x^{ij}, \Delta y^{ij}, \Delta z^{ij}, \Delta^{ij})$ is the difference between the relative hypocentral parameters of the two events, dr^{ij} is the residual between observed and calculated differential travel time of the event pair (i, j), which can be defined as the time difference

$$dr_k^{ij} = (t_k^i - t_j^i)^{obs} - (t_k^i - t_j^i)^{cal} \tag{3.4}$$

And this is the so-called double-difference, I may take advantage of the absolute arrival times of these two events, or use cross-correlation of their seismic waveforms to get the time difference.

If the slowness is not constant, I can have the following relationship after expanding equation 3.3:

$$\frac{\partial t_k^i}{\partial x}\Delta x^i + \frac{\partial t_k^i}{\partial y}\Delta y^i + \frac{\partial t_k^i}{\partial z}\Delta z^i + \Delta\tau^i - \frac{\partial t_k^j}{\partial x}\Delta x^j - \frac{\partial t_k^j}{\partial y}\Delta y^j - \frac{\partial t_k^j}{\partial z}\Delta z^j - \Delta\tau^i = dr_k^{ij} \quad (3.5)$$

Finally, by combining equation 3.5 for all event pairs for a station and for all stations to form a linear system:

$$WGm = Wd \quad (3.6)$$

where matrix **G** contains the partial derivatives of traveltimes with respect to hypocentral parameters and its dimension is $M \times 4N$ (M, the number of double difference observations. N, the number of events). The double differences are contained in the data vector **d**, and **m** is now the change in location and origin time. And **W** is the diagonal weighting matrix comprised of the a priori weights based on the quality of arrival time picks (ranging from 0 to 1).

The approach to find a solution was proposed by Waldhauser and Ellsworth (Waldhauser et al. 2000). It finds the weighted Least Squares (LSQR) solution by using a system of normal equations as follows:

$$\hat{m} = (G^T W^{-1} G)^{-1} G^T W^{-1} d \quad (3.7)$$

where $\hat{\mathbf{m}}$ is the LSQR solution of $\mathbf{m}$.

If the dataset is small and the clusters are well-constrained, Singular Value Decomposition (SVD) method may also be applied to minimize the travel time residuals.

$$\hat{m} = V\Lambda^{-1}GU^{T}d \tag{3.8}$$

where $\mathbf{U}$ and $\mathbf{V}$ are two matrices with the orthonormal singular vectors of the matrix $\mathbf{G}$, and Λ is the diagonal matrix containing the singular values of matrix $\mathbf{G}$.

But when relocating large clusters or many clusters simultaneously, SVD is no longer a reliable option. LSQR can be reliable ([21]) and looks for a solution to the damped Least Squares problem.

$$\left\| W \begin{bmatrix} G \\ \lambda I \end{bmatrix} m - W \begin{bmatrix} d \\ 0 \end{bmatrix} \right\|_2 = 0 \tag{3.9}$$

where I is the identity matrix and m represents the location and time parameter that needs to estimate.

Since only two events are being linked together each time, the sparseness of the G matrix is a major problem when minimizing the travel time residuals. If one event is poorly linked to another, the G matrix can become ill-conditioned, making the solution unstable when using LSQR. This problem can be solved by preprocessing of the data, allowing only well-linked events into the solution process; however, when dealing with moderate number of clusters or data sets, this becomes a complicated problem. In the HYPODD program, LSQR deals with ill-conditioned systems by taking advantage of damping of the solution, where λ is the damping factor in equation (3.3.9). A well-constrained solution to the LSQR problem is essential for reliable earthquake relocations. An assessment of constraints and reliability involves sensitivity testing of the parameters that control HYPODD.

3.3 Determination of velocity structure

To locate an earthquake, one has to determine the optimum values of the earthquake parameters based on minimizing the differences between the observed and the calculated arrival times. For the calculated arrival times, the accuracy depends mostly on how closely the velocity model represents that of the real Earth. For an earthquake, the residuals from all stations can be expressed as RMS (Root Mean Square):

$$RMS = \frac{(\sum_{k=0}^{NS}(residual(k) \times weight(k))^2)^{\frac{1}{2}}}{NP} \tag{3.10}$$

where the residual is the difference between the observed and theoretical arrival times, the weight is a quality factor assigned to a picked phase, NS is the number of stations, and NP is the number of phases used.

Here I adopt the layered velocity model proposed by Maurice Lamontagne (M.Lamontagne 1999) which best describes the velocity structures of south and north bank of St. Laurence Rive, and minimizes the RMS residual for CSZ. The structures and distribution are shown in the following table 3–1 and figure 3–2:

Table 3–1: Layered velocity model

Depth to top(km)	Vp(km/s)
0	5.5
2	5.6
6	6.1
8	6.5
12	6.6
20	6.7
30	6.8
40	8.0

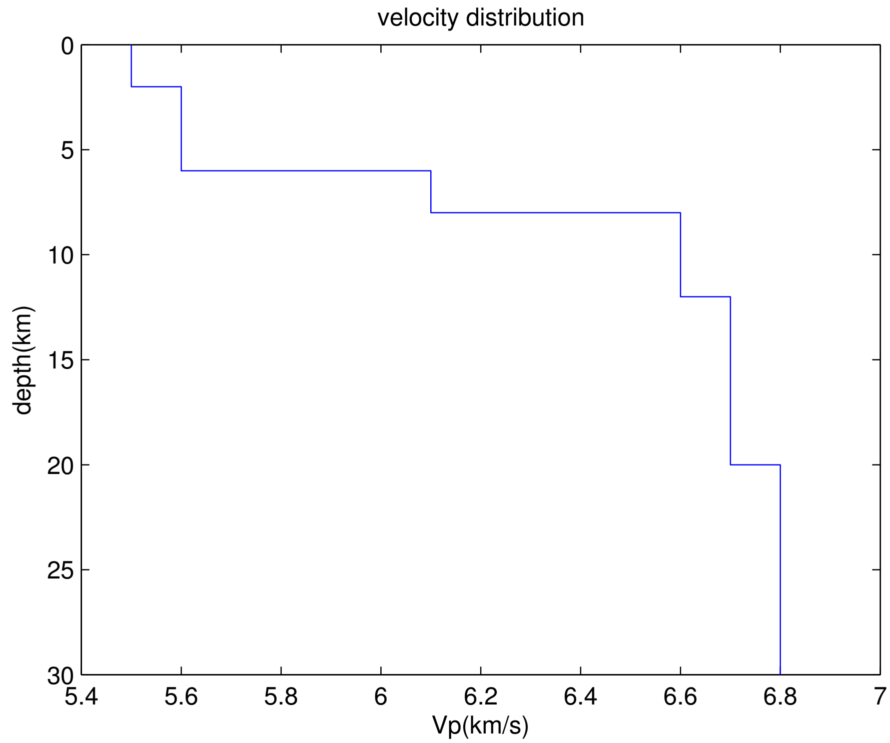

Figure 3–2: P wave velocity model used in my study of CSZ, modified from minimizing the RMS velocity model (Lamontagne, 1999) after testing the individual results of north and south shores

3.4 Waveform cross-correlation Techniques

The accuracy of phase arrivals is the main factor influencing the accuracy of earthquake relocations. I apply a cross-correlation technique to calculate the relative travel times to improve the relocation precision, avoiding the errors from artificial phase picks. It is assumed that the waveform characteristics of two events of similar magnitudes with similar hypocenters and focal mechanisms recorded by a common station are substantially the same. This similarity of waveform shape can give us a high accuracy travel-time difference of these two events both in time and frequency domains. The accuracy of the relative arrival-time readings using waveform cross-correlation methods is much higher than manual pick (a relative timing precision about 1 ms in contrast to routinely manual pick which is 10-30 ms, although picking precision of Pg and Sg phases has changed over the years [9]), and the errors of relocated earthquakes based on such travel-time difference are only a few to tens of meters to a few tens of meters. However, in this thesis, the resolution of the travel-time difference of these event pairs using waveform cross-correlation methods is just 10 ms, because the sampling rate and GPS timing of the digital instruments within the station network of CSZ is 100 Hz since August 1994 (Lamontagne, 1999).

Cross-correlation is very important, particular to S wave, as S wave is much more difficult to be recognized due to the covering up by P tail wave, while S wave is really helpful to identify the focal depth. Even though sometimes the earthquakes are not correctly relocated, the waveform similarity of event pairs can well improve the relative arrival times of general picked phase. I control the distance between event pairs to choose the cross-correlation pairs, based on the fact that similarity of waveforms decays with the degrading interevent separation distance. I use the initial hypocenter locations stored in waveform headfiles to calculate the distance between event pairs. In this thesis, I set the threshold to be 5km according to the one fourth wavelength rule (Geller and Mueller, 1980). This value can include the most related events and control the computational time in an appropriate extent.

I used the correlation detector rather than correlation function as to calculate the time-lapse over the half of cross-correlation time windows (Figure 3–3). I fixed a time window on one seismogram and move another time window on the other seismogram, and do cross-correlation of the parts in two time windows.

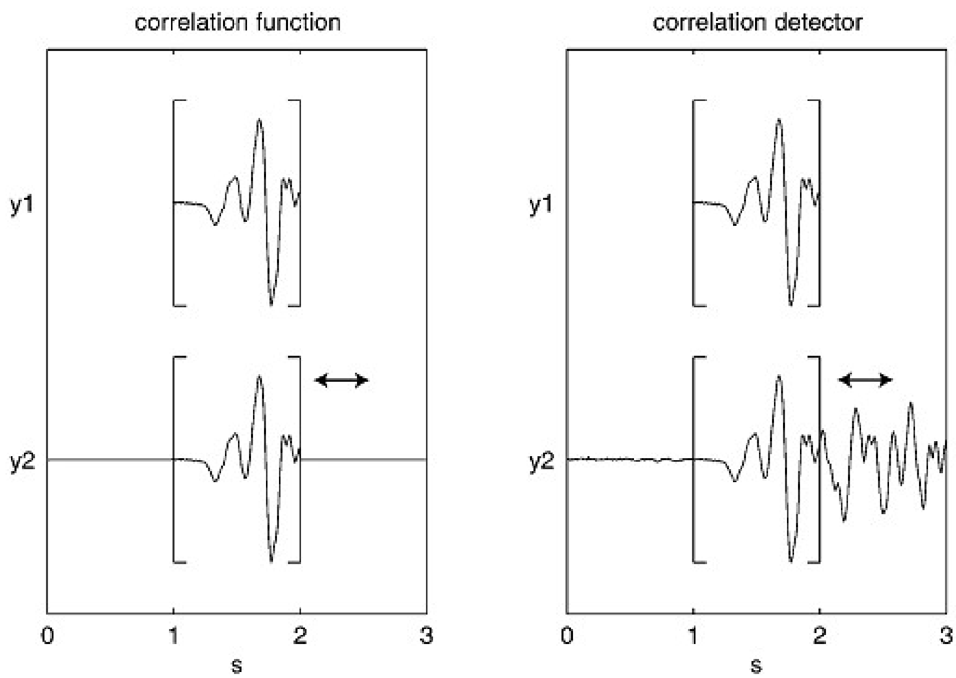

Figure 3–3: Correlation function and correlation detector illustration diagram

As shown in figure 3–3, for correlation function method, the outside part of signal is set zero and correlation function is computed as follows:

$$C(\tau) = c \sum_{n=0}^{N-1} y_1(n) y_2(n+\tau) \tag{3.11}$$

$$c = \left[\sum_{n=0}^{N-1} y_1^2(n) \sum_{n=0}^{N-1} y_2^2(n) \right]^{-\frac{1}{2}} \tag{3.12}$$

where N is the event number of the time window, τ is the delay time and $1 - N \leq \tau \leq N - 1$.

Although conceptually τ can take any value between $1 - N$ and $N - 1$, in fact it should be no more than the half length of window $N/2$. But if the superimposed part of the two time windows is less than half length, the probability of their similarity is only 50%.

In order to improve the range of τ, I apply the cross-correlation detector rather than cross-correlation function, which means that I can use the actual data when sliding the windows. Then, I can set τ any value.

CHAPTER 4
DATA SET AND PROCESSING WORKFLOW

4.1 Introduction to seismic network

The Geological Survey of Canada operates over 150 seismograph stations throughout Canada and produce digital data that is subsequently telemetered to central acquisition systems. Since 1960s when standard network and regional stations was installed, over 50 regional stations are deployed in Canada to provide the most basic seismic information. The telemetered network provide digital data to acquisition systems in the Pacific Geoscience Center (Western Canadian Telemetered Network, WCTN) and Ottawa (Eastern Canadian Telemetered Network, ECTN). Between 1977 and 1988,the Charlevoix seismograph network consisted of a six to seven component vertical short-period analogue network. In November 1988, the Charlevoix local network became the Charlevoix Local Telemetered Network(CLTN), a digital three-component array, aiming at assuring detailed monitoring of the high microearthquake activity in the CSZ.

The earliest microseismicity study near the CSZ was in 1968 (Milne, 1970), and there Ire two other microearthquake surveys following in 1970 and 1974 with stations up to 19, which clearly delineated the CSZ as an active zone (Leblanc et al., 1973). During that time, the observatory was established on the north shore of the St. Lawrence River with a regional station (LMQ) which is installed in 1976 and very important for determining the microearthquake magnitudes in CSZ. In late 1977, a radio-telemetered analog tape recording array of 7 seismometers was deployed to monitor the earthquake activity (Anglin and Buchbinder, 1981). Since 1977, the Charlevoix region has been monitored by a microseismic network of between 6 to 8 stations located on both shores of the St. Lawrence River and a seismograph network consisted of a six to seven component vertical short-period analogue network, which is sufficiently dense for routine hypocenter determinations. In November 1988, the Charlevoix local network became the Charlevoix Local Telemetered Network (CLTN) and data was sampled at 80 Hz. In January 1994, the station LMQ became a digital broadband Canadian National Seismograph Network (CNSN) station, with GPS timing and continuous archival of the data in Ottawa. Finally, every station was updated to a high gain short-period digital instrument with 100Hz sampling rate and GPS timing in August 1994 (Lamontagne, 1999). Table 4–1 shows the details of the stations in this network.

Table 4–1: Stations of Charlevoix Local Telemetered Network (CLTN)

Station code	Latitude	Longitude	Station name
A11	47.2475	-70.1978	Saint Roch-des-Aulnaies
A16	47.4706	-70.0064	Riviére Ouelle
A21	47.7.36	-69.6897	Saint Andre
A54	47.4567	-70.4125	Misere
A61	47.6936	-70.0913	Sainte Mathilde
A64	47.8264	-69.8922	Saint Siméon

So the monitoring of the microseismicity in CSZ was mainly based on this 6-station network (CTLN), one analog seismograph station (LMQ) and one ECTN station (LPQ). And between June and November 1996, Lamontagne deployed additional stations to help define focal mechanisms of micro-earthquakes and to provide constraints on the simultaneous velocity inversion for his PHD dissertation. Nowadays, the CSZ network is still the only eastern Canadian region with dense seismograph network, which detects more than 200 earthquakes every year and is able to calculate the focal depth of the earthquake events.

In this thesis the seismic data from the 19 stations from Canadian National Seismic Network (CNSN) is used to relocate hypocenters over twenty years. This will provide an insight into the seismotectonics and provide a great benefit for earthquake hazard analysis in eastern Canada. Table 4–2 shows the stations that I used in this thesis except the 6 CLTN network stations.

Table 4–2: Stations used in this thesis outside the CLTN network stations

Station Code	Latitude	Longitude
LMQ	47.5485	-70.3258
LPQ	47.3412	-70.0101
A58P	47.5250	-70.2130
A76P	47.6430	-70.2410
A80P	47.5643	-70.5239
A81P	47.4758	-70.3096
A82P	47.6094	-70.3861
BCLQ	46.9263	-71.1728
BLBQ	47.4275	-70.5156
BSPQ	47.4419	-70.5056
DAQ	47.9627	-71.2437
SFA	47.1244	-70.8266
STOQ	47.0188	-71.3795

And figure 4–1 shows the distribution of these 19 stations.

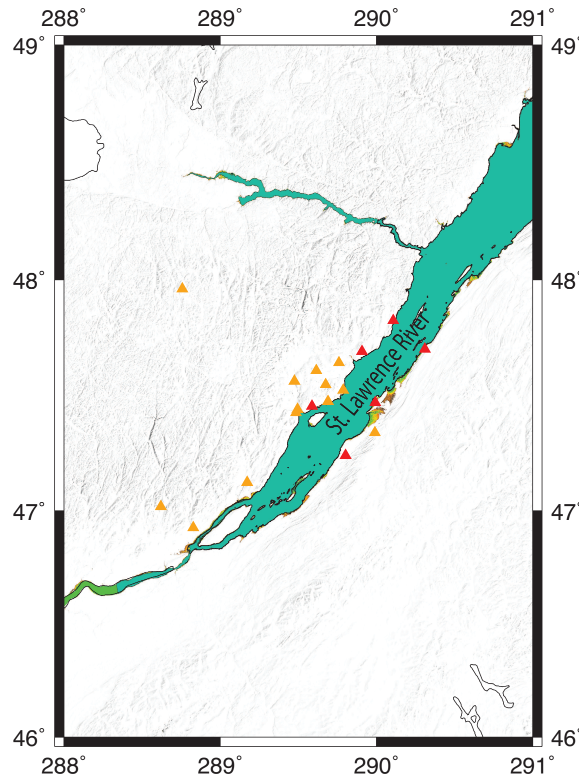

Figure 4–1: Distributions of the seismic stations along St. Lawrence River (green part) in the Charlevoix Seismic Zone, including 6 CLTN stations (red triangles) and other 13 CNSN stations (orange triangles).

4.2 Data and its quality

The data set was obtained for 571 earthquakes with magnitude $mN > 2$ from January 1988 to October 2010 in the Charlevoix Seismic zone (CSZ). This area covers latitudes from $47N$ to $48.5N$ and longitudes from $69W$ to $70.5W$. The following figure 4–2 shows the topography of the target region.

And The following figure 4–3 shows the seismicity of the target region.

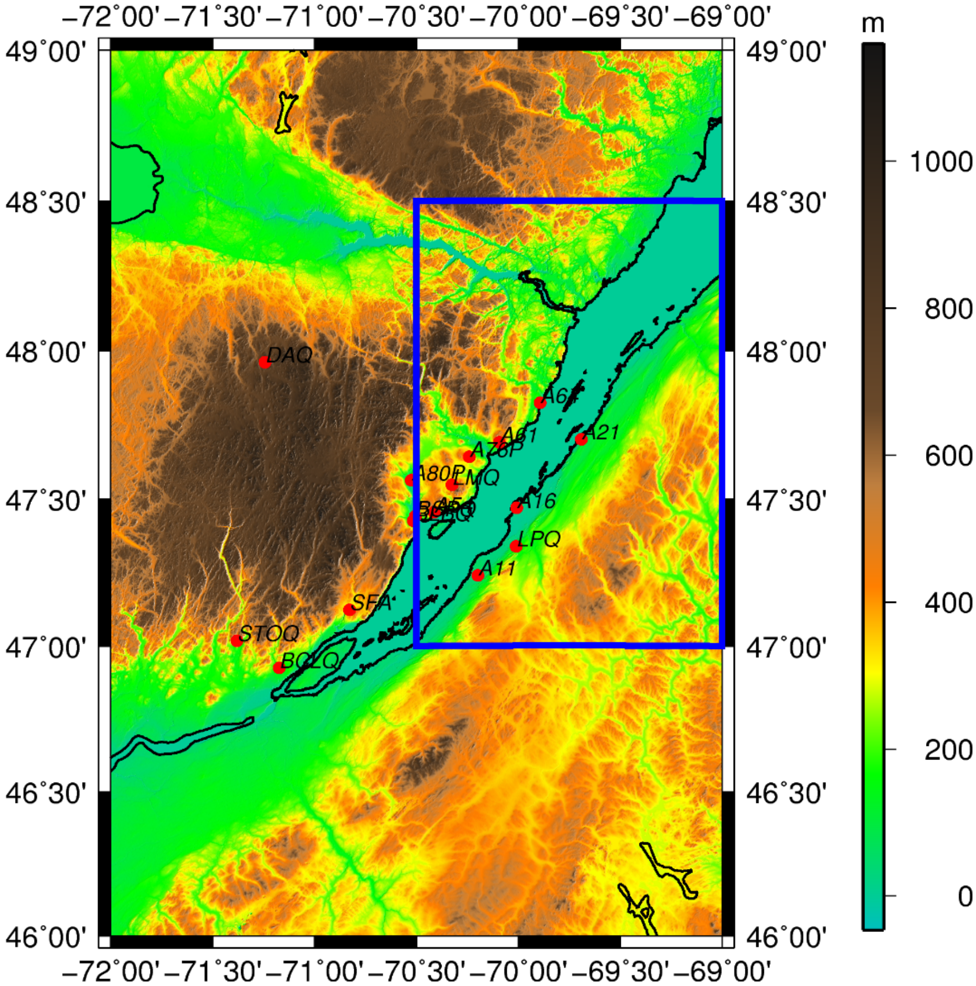

Figure 4–2: Topography of CSZ,boxed area is the study area and red dots are the stations

4.3 HYPODD program and relocation workflow

In this thesis, we use HypoDD program (Waldhauser, 2001) to complement the double-difference relocation algorithms. HypoDD is written in Fortran language, in

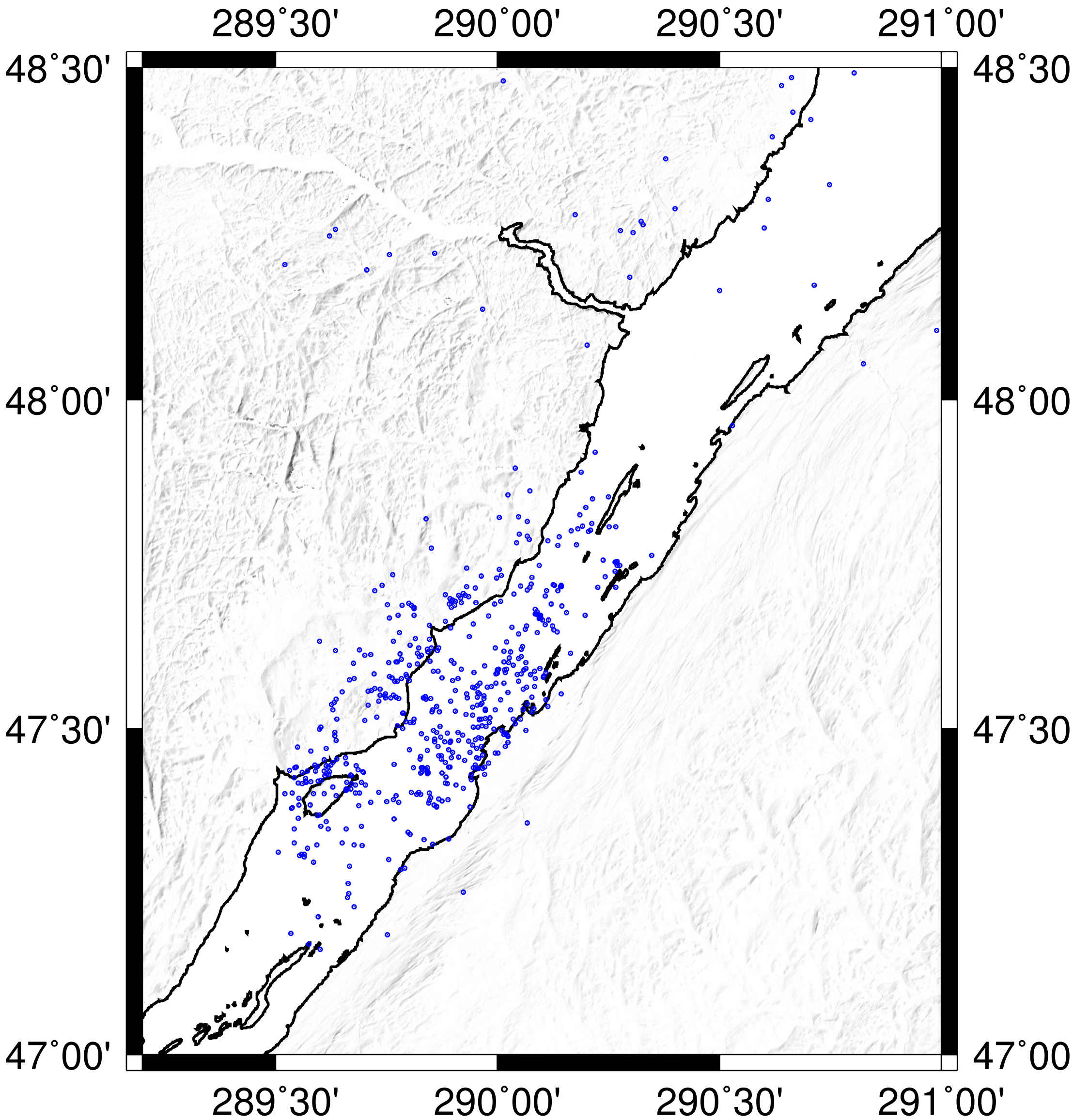

Figure 4–3: Original locations of the earthquakes with magnitude bigger than 2.0, information acquired from CNSN catalog arrival time.

which we can process catalog data or catalog combined with cross-correlation waveform data. It mainly contains two parts: ph2dt and HypoDD. The input files of

HypoDD are dt.ct and dt.cc: dt.ct is the differential time file resulting from the catalog data through ph2dt; while dt.cc is the differential time file resulting from the cross-correlation of waveform data.

There are essentially three steps involved when relocating earthquakes with HYPODD: 1.) the forming of event pairs and links to neighbors, 2.) the forming of clusters, and 3.) double-difference relocation. Figure 4–4 illustrates the workflow of the HypoDD program based on the double-difference relocation algorithms.

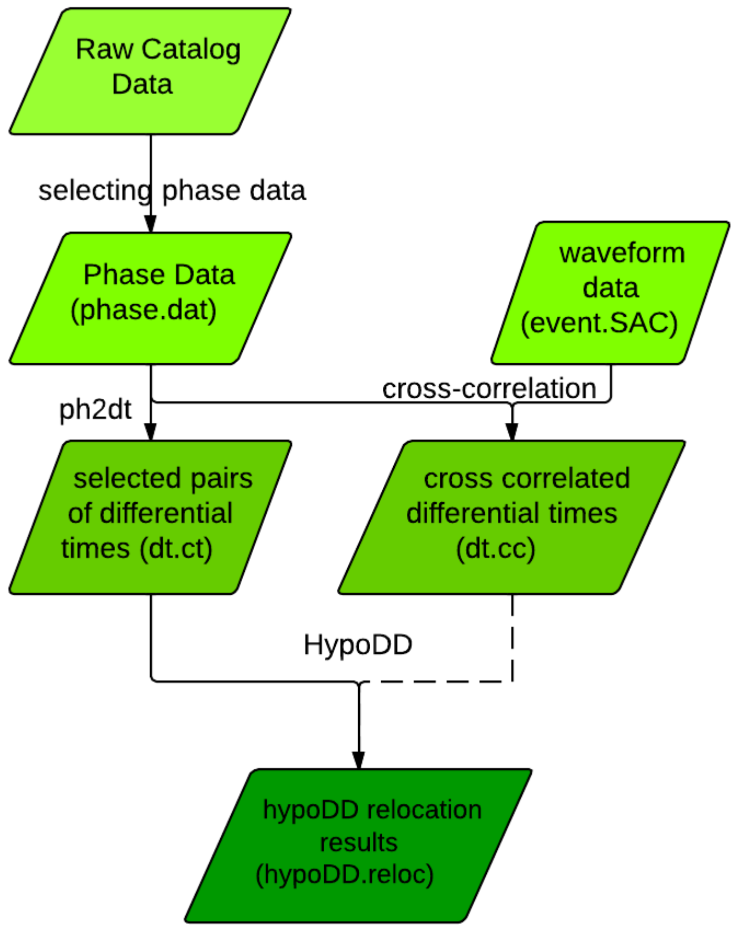

Figure 4–4: The workflow of HypoDD program

4.4 Parameter tests in catalog data processing using ph2dt

The input data of HypoDD program is the travel-difference time of event pairs at seismic stations, which results from either catalog data or waveform data. Ph2dt program establishes links for each event pair to neighbouring event pairs that will ultimately determine clustering during the next step of relocation. In the meantime, it converts the catalog data to the travel-time difference. Hence, the need for appropriate parameter sets is necessary to improve the relocation accuracy when we utilize double-difference relocation algorithm, including the minimum pick weight (MINWGHT), Maximum distance between event pair and station (MAXDIST), Max hypocentral separation between event pairs (MAXSEP), Max number of neighbours per event (MAXNGH), Min. number of links required to define a neighbour (MINLNK), Min. number of links per pair saved (MINOBS) and Max number of links per pair saved (MAXOBS). The tables of parameter tests are from the HypoDD results based on the catalog data of my Charlevoix study area since January 1st, 1988 to October 30th, 2010, which give us a clear impression how these parameters will affect the errors of relocated earthquakes.

MINWGT: Minimum pick weight allowed to be eligible for data processing. Table 4–3 shows the results of different MINWGT values. We noticed that the difference is not obvious, errors and events relocated are the same when increasing it from 0 to 0.5, but when increased to 1, the number of events relocated reduced to 2542, so we take MINWGT= 0.5 as the optimal value for this parameter.

Table 4–4shows the results of test on this parameter. From this table we can see that relocation results when MAXDIST is 60 km are best because the total error

Table 4–3: Parameter test on different MINWGT values

MINWGHT	dx	dy	dz	Total error (m)	Events
0	33	31	57	72.79423054	2544
0.5	33	31	57	72.79423054	2544
1	33	31	58	73.57988856	2542

dx : hypocentral error in EW direction; dy : hypocentral error in NS direction; dz : hypocentral error in vertical direction; total: total hypocentral error

keeps decreasing when increasing to this value and the number of events starts to decrease when increasing from this value.

Table 4–4: Parameter test on different MAXDIST values

MAXDIST(km)	dX(m)	dY(m)	dZ(m)	Total(m)	Events
200	43	40	96	112.5388822	2533
150	43	40	96	112.5388822	2533
140	43	40	96	112.5388822	2533
130	43	40	96	112.5388822	2533
120	43	40	96	112.5388822	2533
110	43	41	97	113.7497253	2535
100	43	41	84	102.8882889	2537
90	40	37	77	94.32921075	2536
80	40	36	75	92.30926281	2531
70	39	36	76	92.6984358	2530
60	38	33	71	87.02873089	2532
50	36	32	66	81.70679286	2508
40	27	24	45	57.70615219	2484
35	15	13	14	24.2899156	2194
30	7	7	6	11.5758369	1718

MAXSEP: Maximum hypocentral separation. Table 4–5 shows the test on this parameter. From this we can see that along with the increase of this value, the maximum hypocenteral separation is increased and more events are included in the same cluster and generate more event pairs. Therefore, relocated events get more, while the error gets bigger more or less. We select MAXSEP = 5 km when the number of events is rather big and the error is rather small. The relocation performance become best at this point, as there are relative more relocated events and relative smaller error value.

Table 4–5: Parameter test on different MAXSEP values

MAXSEP	dX	dY	dZ	Total	Events
10	38	33	71	87.02873089	2532
9	37	33	72	87.4185335	2530
8	37	33	72	87.4185335	2531
7	37	34	73	88.62279616	2524
6	37	34	74	89.4483091	2502
5	37	33	69	84.96469855	2473
4.5	36	33	72	87	2448
4	37	33	69	84.96469855	2409
3.5	36	32	68	83.33066662	2269
3	35	31	67	81.70067319	2109

MAXNGH: Maximum number of neighbors allowed per event. In fact this setting is for reducing the computation burden such that the computing time can be shortened when processing a large dataset. In this test, we have 547 events so we can run test on MAXNGH=547, and then test other smaller values. The results are shown in the following Table 4–6.

Table 4–6: Parameter test on different MAXNGH values

MAXNGH	dX	dY	dZ	Total	Events

150	48	46	101	120.9173271	2451
70	46	44	101	119.3859288	2454
60	46	46	97	116.7946917	2452
50	45	44	97	115.6287162	2450
40	45	44	96	114.7911146	2465
30	43	42	90	108.2266141	2456
25	43	40	85	103.3150521	2466
24	42	39	87	104.1825321	2463
23	42	40	86	103.7304198	2452
22	41	38	84	100.9009415	2457
21	41	38	82	99.24212815	2463
20	40	38	84	100.4987562	2461
19	40	37	82	98.45303449	2459
18	39	37	83	98.88882647	2462
17	38	36	80	95.60334722	2463
16	39	36	83	98.51903369	2460
15	38	36	81	96.44169223	2460
14	28	25	76	84.76437931	2461
13	37	34	75	90.27735043	2469
12	38	35	74	90.24965374	2472
11	38	34	74	89.86656775	2478
10	37	33	69	84.96469855	2473

9	36	33	70	85.35221145	2472
8	36	33	68	83.71977066	2475
7	36	33	66	82.1035931	2468
6	36	32	66	81.70679286	2470
5	36	34	65	81.71291208	2465
4	35	32	56	73.38255924	2449
3	33	31	51	68.19824045	2435
2	29	26	43	58.01723882	1835

MINLNK: Minimum number of links required to define a neighbor. Table 4–7 shows the tests I ran to see the influence of different MINLNK parameters. We can tell that 7 is the optimal one because the total error is smallest and the number of events is almost at the top level.

MINOBS: Minimum number of links per pair saved. This parameter is set to reduce computing and storage burden too. The smaller we set, the bigger data set we would have and the longer HypoDD would take. Here we take 2 as optimal parameter because the total error is smallest and the number of events is almost at the top level.

MAXOBS: Maximum number of links per pair saved. This parameter controls the max number of observations to be selected for each event pair. The larger MAXOBS is, the more observations we would have for each event pair. Table 4–9

Table 4–7: Parameter test on different MINLNK values

MINLNK	dX	dY	dZ	Total	Events
10	37	35	70	86.56789243	2521
9	36	34	67	83.3126641	2528
8	36	33	66	82.1035931	2527
7	36	33	66	82.1035931	2532
6	36	33	68	83.71977066	2533
5	36	34	68	84.11896338	2528
4	36	33	68	83.71977066	2530
3	36	33	68	83.71977066	2528
2	36	33	69	84.53401682	2524
1	36	33	69	84.53401682	2525

Table 4–8: Parameter test on different MINOBS values

MINOBS	dX	dY	dZ	Total	Events
10	36	34	71	86.56211643	2241
9	36	33	72	87	2351
8	36	32	72	86.62563131	2458
7	36	33	72	87	2477
6	36	33	69	84.53401682	2520
5	36	32	66	81.70679286	2527
4	35	33	67	82.48030068	2532
3	36	33	66	82.1035931	2531
2	35	33	66	81.67006796	2532
1	36	33	66	82.1035931	2532

shows the tests I ran with different MAXOBS values, we select 11 to be the optimal value because it gives rather small error and the relocated events are quite many.

Table 4–9: Parameter test on different MAXOBS values

MAXOBS	dX	dY	dZ	Total	Events
100	35	33	66	81.67006796	2532
75	35	33	66	81.67006796	2532
50	35	33	66	81.67006796	2532
25	35	33	66	81.67006796	2532
15	36	33	67	82.90958931	2532
14	36	33	66	82.1035931	2532
13	36	32	64	80.09993758	2535
12	35	33	64	80.0624756	2538
11	33	31	59	74.37069315	2546
10	33	30	52	68.50547423	2544
9	24	25	31	46.49731175	2540
8	21	22	26	40.01249805	2523

4.5 Earthquakes relocated by HypoDD with catalog data only

After analysis using ph2dt, strongly linked event-pairs have been identified and recorded, and can serve as input to HYPODD for the double-difference relocations. HYPODD first groups the event-pairs into clusters. A cluster can be as small as two earthquakes (one event-pair) or as large as the whole event set. A cluster is a continuous chain of event-pairs that are strongly linked and meet user defined criteria set forth in the HYPODD input, by the values of WDCT or DIST. It is possible and likely that two clusters may be extremely close to each other and still be two separate clusters rather than one larger cluster. Depending on the input parameters, HYPODD may form a few large clusters with many events in them or several small clusters with a smaller number in each one; this is determined by the pre-specified values, such as MAXSEP or WDCT. HYPODD can relocate all of the clusters or a selected sub-set of clusters.

The relocation process proceeds by iterative reduction of double difference travel time residuals. The number of iterations is specified by the user, who considers the size of the data set and the size of the clusters. Weights are determined for P and S waves and assigned to a certain number of iterations. Weights can be reset for each iteration. There can be any combination of the number of user specified iterations and weighting. Also included in the iteration process are the parameters WDCT and WDCC, which are the maximum event separation, in kilometers, for the catalog and cross-correlated data, respectively. These parameters are similar to MAXSEP in the ph2dt program, however, MAXSEP is the maximum distance between neighboring event-pairs and WDCT is the maximum distance between two hypocenters to form event pairs. Considering the similarities between these two parameters in conjunction with the station and hypocenter spacing in the Charlevoix Seismic Zone, in order to maintain consistency, MAXSEP and WDCT were always set equal to each other in this study. Damping is used only when LSQR is the option chosen for inversion.

Table 4–10: Weighting scheme for relocation with catalog data only, parameters are used in hypoDD package.

iterations	A priori, P-wave WTCTP	A priori, S-wave WTCTS	Misfit weight (residual cutoff) WRCT	Dist weight (separation) WDCT	DAMP
1-4	1	0.5	-9	5	40
5-8	0.1	0.05	6	5	80
9-12	0.1	0.05	6	5	100

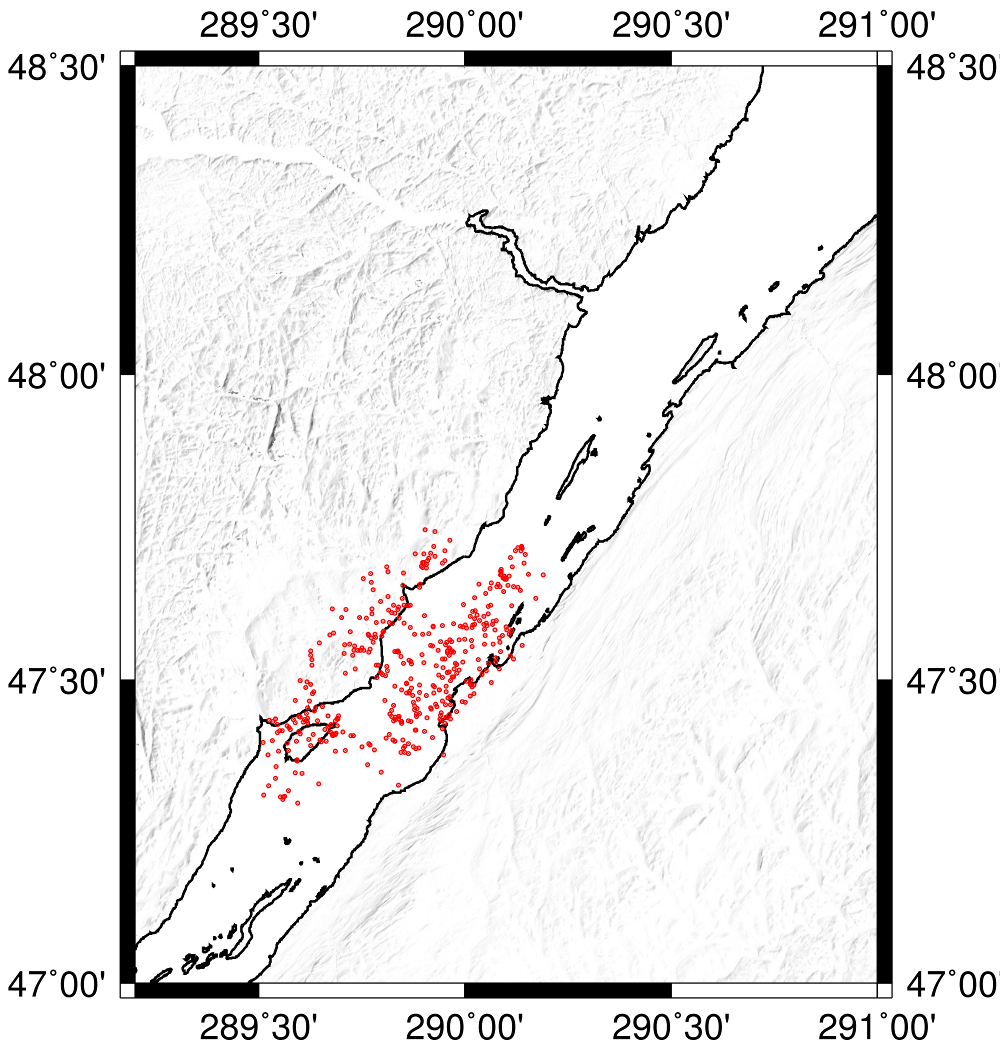

Figure 4–5: Relocations of the earthquakes with magnitude larger than 2.0, processing only using the catalog arrival times using the HypoDD package

4.6 Earthquakes relocated by HypoDD with catalog and cross-correlated data

The cross correlated data is generated by the algorithm described in Chapter 3.4, after filtering the data by magnitude larger than or equal to 2, we get the cross-correlated differential travel time file, dt.cc. Together with dt.ct data which is generated by ph2dt, we ran HypoDD again with the following input parameter file which specifies that the data we use consists of catalog differential time data and cross correlation differential time data as well.

And the epicentral plot of the relocations adopting these two data set is shown in Fig 4–6

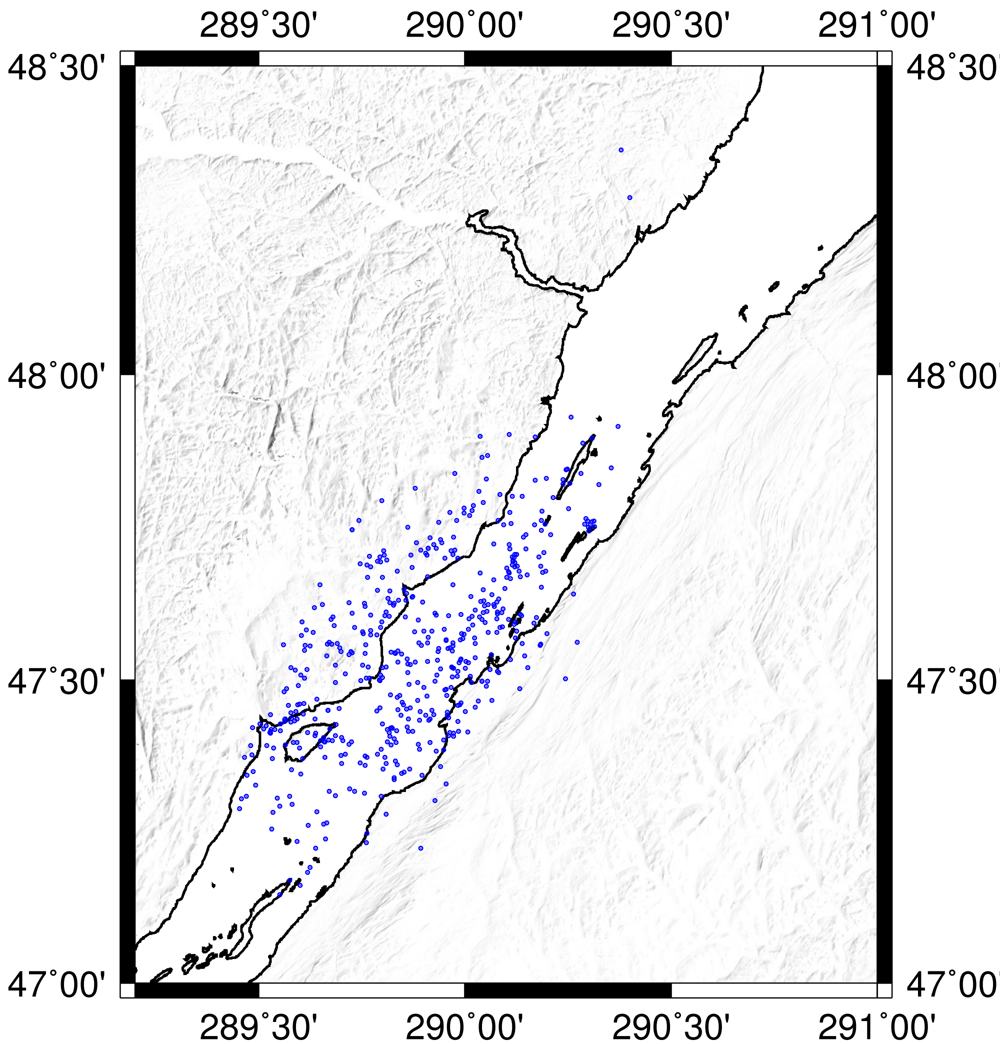

Figure 4–6: Relocations of the earthquakes with magnitude bigger than 2.0, processing both catalog arrival time and cross correlated data using HypoDD packages

CHAPTER 5
Relocation Results and Discussions

5.1 Charlevoix Seismicity

In my thesis, I acquired the catalog and waveform records of magnitude greater than 2.0 earthquakes in Charlevoix Seismic Zone from the CNSN since January 1st 1988 to October 30th 2010. I successfully relocated 497 events with only catalog data and relocated 469 events with cross-correlation technique from the 571 initial events by applying HypoDD program based on the double-difference relocation algorithms. Most of the earthquakes are concentrated along the shores of St. Laurence River (Figure 5–1).

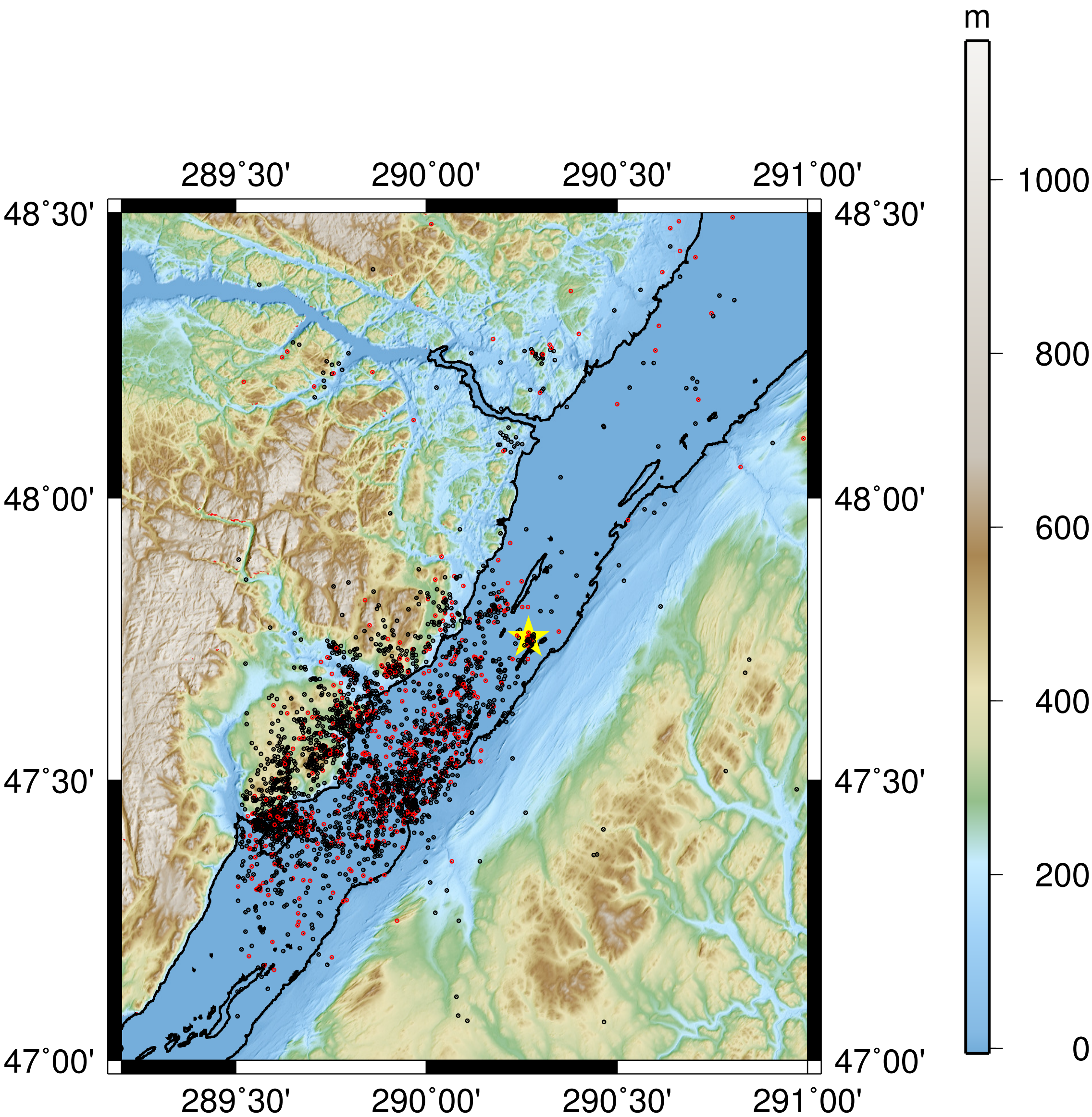

Figure 5–1: Relocations of all the earthquakes, processing only catalog arrival time using HypoDD packages. The yellow star stands for a big earthquake(Mag > 5) and the black ones stand for earthquakes of magnitude ranging from -0.2 to 2.

5.2 Relocation results and comparison

Following figure 5–2 is the epicentral plot of relocation results with catalog data only(5–2(a)) and with both catalog and cross correlated data(5–2(b)). Comparing these two figures, the result above shows that relocation with both data set is more spread out than the relocation result with catalog data only.

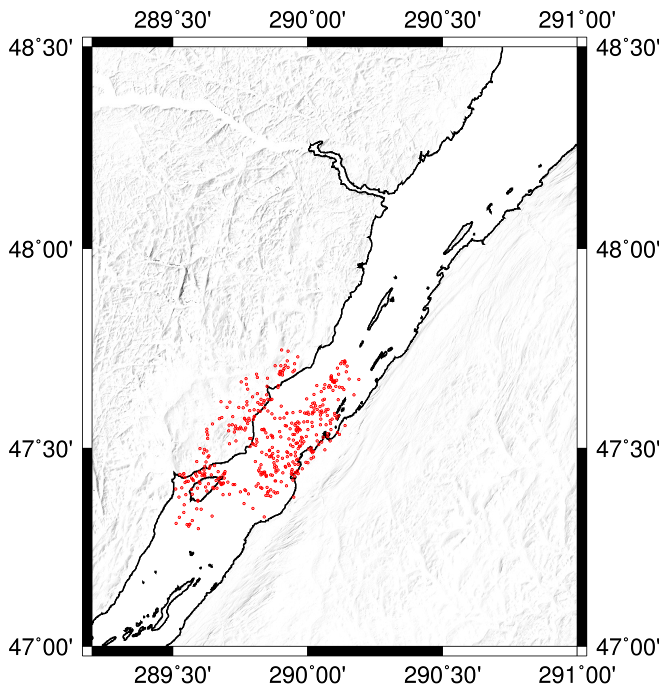

(a) Relocation results with catalog arrival time

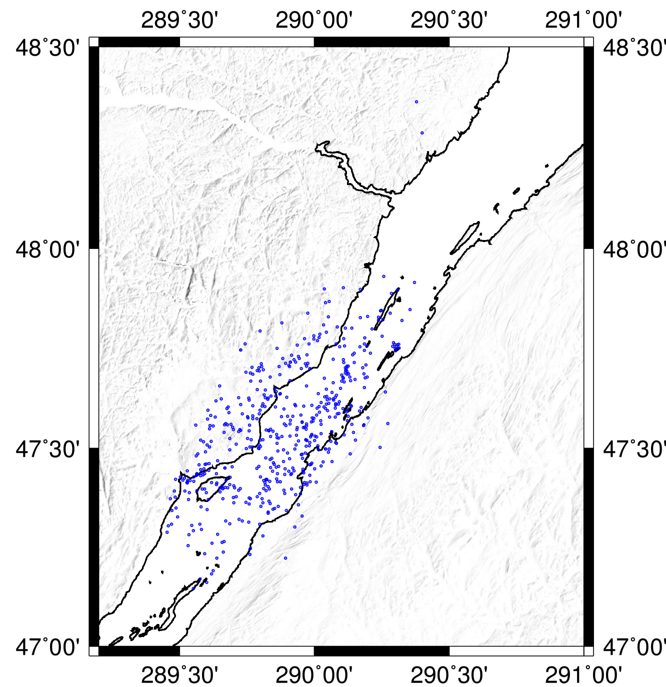

(b) Relocation results with both catalog arrival time and cross correlated data

Figure 5–2: Comparison of relocation results

And the table 5–1 shows the mean shift of locations during each LSQR iteration, where x direction stands for the east-west direction, y stands for north-south direction and z stands for vertical direction. It is shown from this table that the two groups of pre- and post- relocation have average shifts of 298.4 meters in east-west direction, 237.4 meters in north-south direction and 558.1 meters in vertical depth.

Table 5–1: The mean shift changes along with iteration number in HYPODD program

iteration	mean shift in x(m)	mean shift in y(m)	mean shift in z(m)
1	0.2	-0.4	-6.6
2	-205.2	-162.5	-337.5
3	-46.6	-43.6	-82.2
4	-15.3	-12.3	-45.6
5	-15.2	-3.7	-67.2
6	-3.9	-5.1	-6.7
7	-3	-3	-2.4
8	-1.9	-1.8	-2.4
9	-5.2	-3.4	-6.9
10	-0.7	-0.4	0.0
11	-0.8	-0.5	-0.8
12	-0.8	-0.7	0.2
total	-298.4	-237.4	-558.1

5.3 Relocation cross section results and comparison

5.3.1 Cross section in Northeastern CSZ

Fig 5–3 and 5–4 show the comparison of the same cross section plots in northeastern part of CSZ, located in both shores of St. Laurence River:

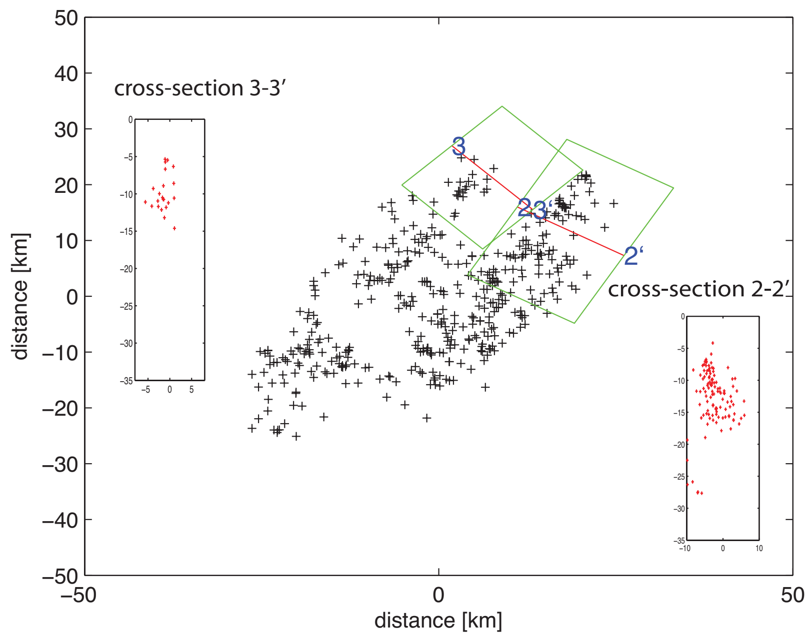

Figure 5–3: Cross section plot with catalog data, northeastern CSZ

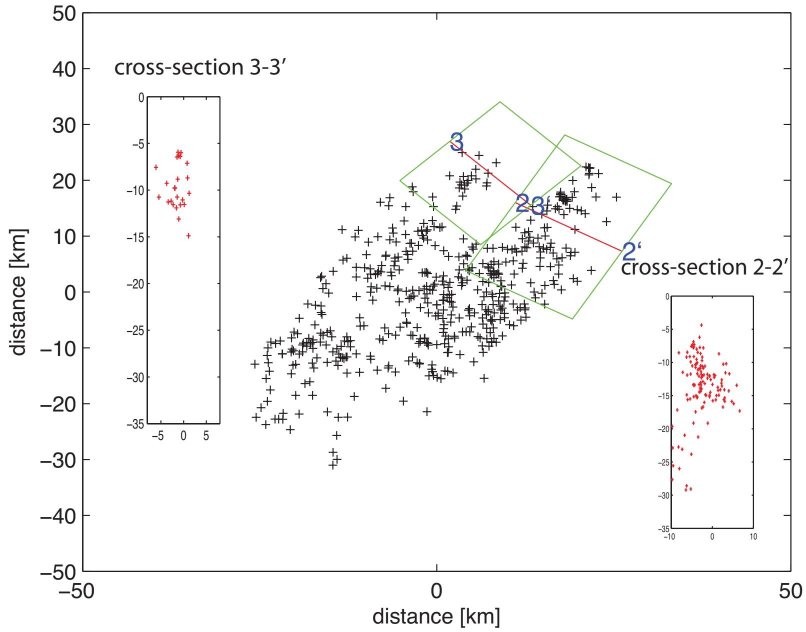

Figure 5–4: Cross section plot with both catalog data and cross correlated data, north-eastern CSZ

From these two figures we can tell that the minor fault feature revealed by the cross section plot is more obvious in relocation with cross correlation and catalog data.

5.3.2 Cross section in central CSZ

Fig 5–5 and 5–6 show the comparison of the same cross section plots in central part of CSZ, located in both shores of St. Laurence River:

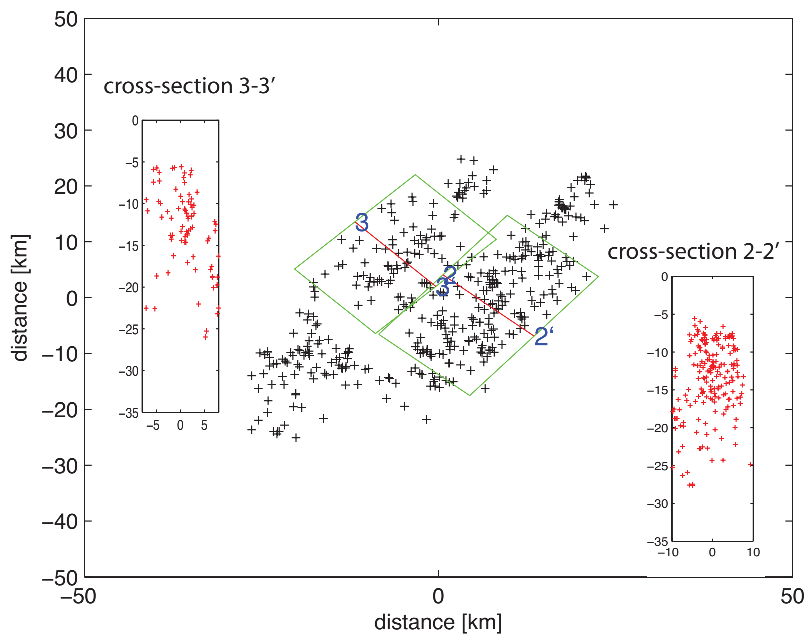

Figure 5–5: Cross section plot with catalog data, central CSZ

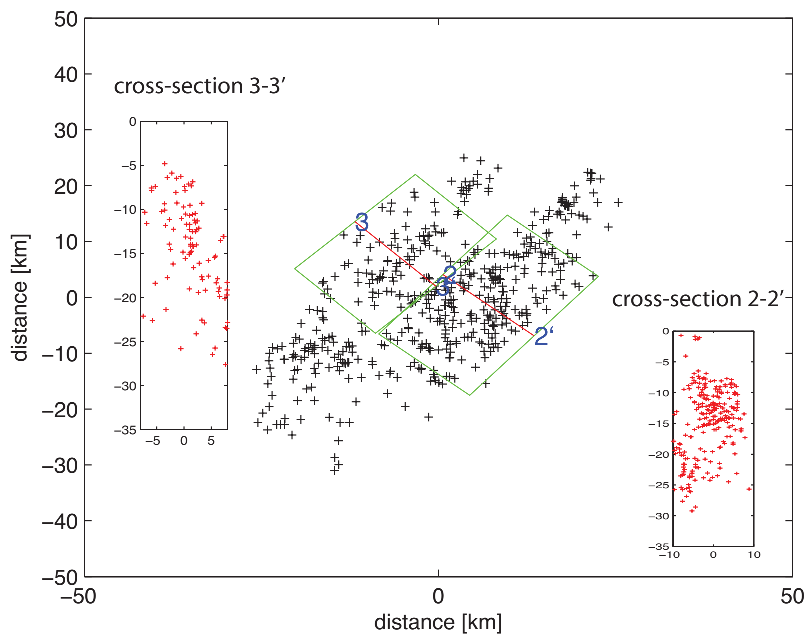

Figure 5–6: Cross section plot with both catalog data and cross correlated data, central CSZ

5.3.3 Cross section in Southwestern CSZ

Fig 5–7 and 5–8 show the comparison of the same cross section plots in southwestern part of CSZ, located in both shores of St. Laurence River:

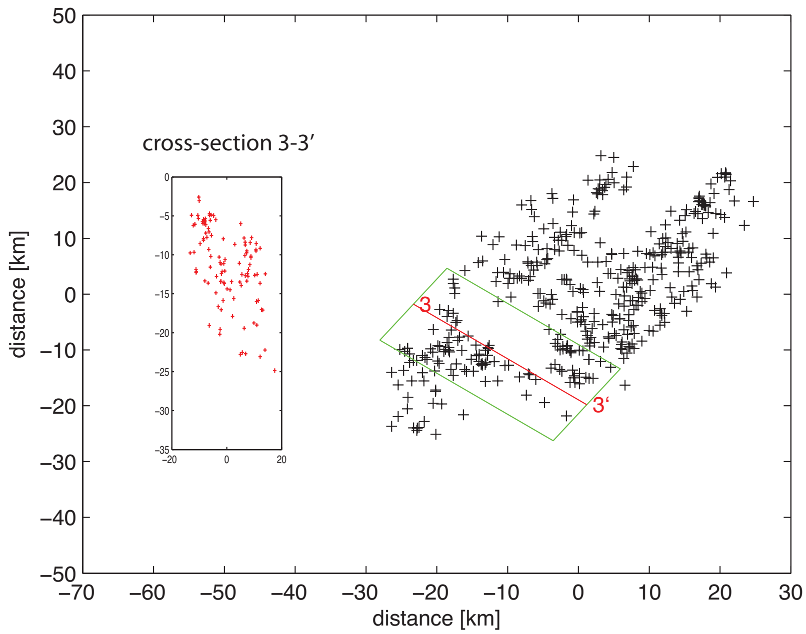

Figure 5–7: Cross section plot with catalog data, southwestern CSZ

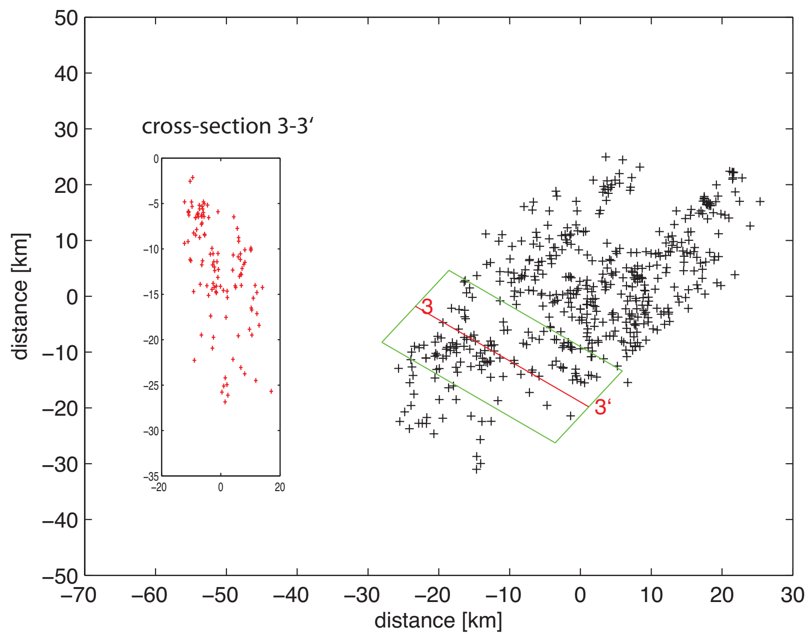

Figure 5–8: Cross section plot with both catalog data and cross correlated data, southwestern CSZ

In the Northeastern part of CSZ, we can tell there is a minor fault features in the south shore of the Saint Laurence River, dipping about 62 degrees to the southeast.

5.4 Conclusions

All CSZ earthquakes occur within the Precambrian basement (Leblanc and Buchbinder, 1977), which is cut by faults created during four major tectonic events. However, the geological structures of the seismogenic Precambrian basement under the St. Lawrence River, are hidden by several kilometres of Appalachian nappes (Lyons et al., 1980) and hundreds of meters of Quaternary sediments. Although quite a few scientists have studied the CSZ by applying various geophysical methods, the elaborate geological feature of this area is still not well understood.

In this thesis, we use the HypoDD program based on the double-difference relocation algorithms to successfully 497 events with only catalog data and relocated 469 events with cross-correlation technique from the 571 initial events in Charlevoix Seismic Zone from January 1988 to October 2010, adopting the 1-D layered velocity model on both shores of Saint Laurence River (Lamontagne, 1999). From the relocation cross sections, we can find the minor rift fault geological features are very obvious in the CSZ northeast part. It shows a fault dipping about 62° to the southeast, whereas the central and southern cross-sections are so scattered that we are not to be able to find fault features clearly. From previous study on CSZ, we know that to the north of the CSZ, the plateau is cut by a series of EW normal faults related to the creation of the Saguenay Graben in late Precambrian to Ordovician (700-500Ma). Along the St. Lawrence River, low relief generally corresponds to the hanging wall of normal faults of similar age (Lamontagne, 1999).

These preliminary relocations for Charlevoix Seismic Zone indicate that fault features are more easily defined in the northeastern part of the zone. In contrast, the geological features are more complex and difficult to identify in the southwestern part. Therefore, the geological structure of Charlevoix seismic zone is complex and highly fractured. There may be some minor fault feature structures but not a major fault, so our hypocentral results are scattered.

CHAPTER 6
Summary and future work of Charlevoix Seismic Zone

In this thesis, according to the seismic data acquired from Canadian National Seismograph Network, I apply he double-difference relocation algorithms to relocate the micro earthquakes of Charlevoix Seismic Zone in the almost past twenty years(1988.01-2010.10). And this method can help me to find some minor geological structures in the Charlevoix Seismic Zone. The main results of my thesis is list below:

* successfully 497 events with only catalog data and relocated 469 events with cross-correlation technique from the 571 initial events.
* comparison of the earthquake original locations and relocations in the scales of geometry and cross section.
* find a minor rift fault geological features dipping about 62 degree in the CSZ northeast part.
* the geological structure of Charlevoix seismic zone is complex and highly fractured, especially difficult to identify in the southwest.

Although I have got some preliminary results for Charlevoix Seismic Zone, there are a few aspects need to be improved, for example, analysis about the effect of distribution of station network on relocation results. In fact, I have started to use waveform cross-correlation method to relocate the micro earthquakes in the Charlevoix Seismic Zone. However, the results look still scattered because of the poor quality of seismic waveform records of this area. Now I am trying to improve the seismic signal quality and manually assign weights for the picks based on the the quality of fist arrival. By the waveform cross-correlation technique, it is possible to calculate more accurate travel-time difference, in order to make the relocations more precise. Meanwhile, I will calculate the focal mechanisms to get more distinct fault features and also analyze the field stress variations in the Charlevoix Seismic Zone. I will rank the seismograms along with the epicentre distance in order to pick up more useful phases for further improving the accuracy of earthquake locations. A better understanding of the fine-scale geological structures in the Charlevoix Seismic Zone can be achieved by more accurate seismicity locations. At the same time, high accuracy earthquake location and more phase information will provide foundation for the other research in seismology.

References

[1] John Adams and Gail Atkinson. Development of seismic hazard maps for the proposed 2005 edition of the national building code of canada. *Canadian Journal of Civil Engineering*, 30(2):255–271, 2003.

[2] John Adams and Peter Basham. The seismicity and seismotectonics of canada east of the cordillera. *Geoscience Canada*, 16(1), 1989.

[3] John Adams and Peter Basham. The seismicity and seismotectonics of eastern canada. *Neotectonics of North America*, 1:261–276, 1991.

[4] FM Anglin. Seismicity and faulting in the charlevoix zone of the st. lawrence valley. *Bulletin of the Seismological Society of America*, 74(2):595–603, 1984.

[5] Allison L Bent, Janet Drysdale, and HK Claire Perry. Focal mechanisms for eastern canadian earthquakes, 1994–2000. *Seismological Research Letters*, 74(4):452–468, 2003.

[6] GGR Buchbinder, A Lambert, RD Kurtz, DR Bower, FM Anglin, and J Peters. Twelve years of geophysical research in the charlevoix seismic zone. *Tectonophysics*, 156(3):193–224, 1988.

[7] John F Cassidy. A comparison of the receiver structure beneath stations of the canadian national seismograph network. *Canadian Journal of Earth Sciences*, 32(7):938–951, 1995.

[8] P Castaigne, B Pertuiset, P Rondot, and J De Recondo. Ataxie optique dans les deux hémichamps visuels homonymes gauches après exérèse chirurgicale dun anévrysme artériel de la paroi du ventricule latéral. *Rev Neurol (Paris)*, 124(4):261–268, 1971.

[9] Robert J Geller and Charles S Mueller. Four similar earthquakes in central california. *Geophysical Research Letters*, 7(10):821–824, 1980.

[10] Quebec. Direction Des Leves Geoscientifiques and J Rondot. *Reconnaissances géologiques dans Charlevoix-Saguenay.* 1979.

[11] Stephen Halchuk and John Adams. Deaggregation of seismic hazard for selected canadian cities. In *Proceedings of the 13th World Conference on Earthquake Engineering, Vancouver, Canada. Paper*, volume 2470, 2004.

[12] Paul F Hoffman. Precambrian geology and tectonic history of north america. *The Geology of North America*, pages 447–512, 1989.

[13] Thomas S James and Allison L Bent. A comparison of eastern north american seismic strain-rates to glacial rebound strain-rates. *Geophysical Research Letters*, 21(19):2127–2130, 1994.

[14] SL Kamo, TE Krogh, and PS Kumarapeli. Age of the grenville dyke swarm, ontario-quebec: implications for the timing of lapetan rifting. *Canadian Journal of Earth Sciences*, 32(3):273–280, 1995.

[15] M Lamontagne. *New and revised earthquake focal mechanisms of the Charlevoix seismic zone, Canada*. Geological Survey of Canada, 1998.

[16] Maurice Lamontagne. *Rheological and geological constraints on the earthquake distribution in the Charlevoix Seismic Zone, Quebec, Canada*. 1999.

[17] Maurice Lamontagne and Giorgio Ranalli. Faults and spatial clustering of earthquakes near la malbaie, charlevoix seismic zone, canada. *Seismological Research Letters*, 68(2):337–352, 1997.

[18] G Leblanc and G Buchbinder. Second microearthquake survey of the st. lawrence valley near la malbaie, quebec. *Canadian Journal of Earth Sciences*, 14(12):2778–2789, 1977.

[19] G Leblanc, AE Stevens, RJ Wetmiller, and R DuBerger. A microearthquake survey of the st. lawrence valley near la malbaie, quebec. *Canadian Journal of Earth Sciences*, 10(1):42–53, 1973.

[20] Yvon Lemieux, Alain Tremblay, and Denis Lavoie. Structural analysis of supracrustal faults in the charlevoix area, quebec: relation to impact cratering and the st-laurent fault system. *Canadian Journal of Earth Sciences*, 40(2):221–235, 2003.

[21] Christopher C Paige and Michael A Saunders. Lsqr: An algorithm for sparse linear equations and sparse least squares. *ACM Transactions on Mathematical Software (TOMS)*, 8(1):43–71, 1982.

[22] Jehan Rondot. La structure de charlevoix comparée à d'autres impacts météoritiques. *Canadian Journal of Earth Sciences*, 7(5):1194–1202, 1970.

[23] Gordana Vlahovic, Christine Powell, and Maurice Lamontagne. A three-dimensional p wave velocity model for the charlevoix seismic zone, quebec, canada. *Journal of Geophysical Research: Solid Earth (1978–2012)*, 108(B9), 2003.

[24] Felix Waldhauser and William L Ellsworth. A double-difference earthquake location algorithm: Method and application to the northern hayward fault, california. *Bulletin of the Seismological Society of America*, 90(6):1353–1368, 2000.

[25] Patrick Wu. Effect of viscosity structure on fault potential and stress orientations in eastern canada. *Geophysical Journal International*, 130(2):365–382, 1997.

[26] Patrick Wu and Henry S Hasegawa. Induced stresses and fault potential in eastern canada due to a realistic load: a preliminary analysis. *Geophysical Journal International*, 127(1):215–229, 1996.

APPENDIX A
Appendix A List of all events

Date	Time	Latitude	Longitude	Depth(km)	Magnitude(mN)	ID
19880425	18281660	47.4640	-70.1010	19.9	2.0	1005
19880508	07390110	47.4410	-70.0290	08.5	2.0	1006
19880625	18370690	47.6900	-70.1080	05.0	2.0	1008
19880917	07295740	47.4380	-70.1640	07.7	2.0	1016
19890102	02424770	47.1702	-70.4246	09.5	2.0	1018
19890227	15072750	47.5262	-70.1474	18.0	2.0	1020
19890228	22125070	48.2570	-70.3650	00.0	2.0	1021
19890321	12511160	47.5636	-70.0225	09.8	2.0	1026
19900303	15175410	47.6990	-70.0829	08.4	2.0	1044
19910601	04492730	47.4679	-70.1991	08.8	2.0	1067
19920130	10423340	47.5389	-70.0349	06.0	2.0	1080
19920315	07454710	47.7187	-69.8561	10.2	2.0	1082
19920316	07223550	47.2482	-70.3349	08.6	2.0	1083
19920406	17260440	47.4564	-70.0871	10.9	2.0	1085
19920827	22191810	47.6847	-70.1873	00.0	2.0	1094
19920908	20480010	47.4888	-70.3667	07.3	2.0	1095
19921203	10020790	47.6099	-70.1753	11.8	2.0	1097
19930823	09312680	47.5603	-69.9423	11.9	2.0	1112

Date	Time	Latitude	Longitude	Depth(km)	Magnitude(mN)	ID
19940207	06090140	47.5903	-70.0005	08.4	2.0	1118
19940322	23342450	47.5257	-69.9231	14.9	2.0	1120
19940723	09464120	47.3804	-70.1365	15.2	2.0	1125
19950222	16390560	47.4633	-70.0055	19.3	2.0	1131
19950503	14315350	47.6769	-69.8451	11.2	2.0	1133
19950616	12222300	47.3937	-70.4469	06.4	2.0	1136
19950731	03200310	47.5314	-69.9181	09.7	2.0	1138
19951026	19312610	47.4189	-70.4204	05.3	2.0	1147
19960105	04403020	47.6017	-70.2251	05.8	2.0	1151
19960505	13221920	47.4337	-70.4402	14.4	2.0	1158
19960526	16414950	47.5617	-70.2772	10.6	2.0	1160
19960704	12270740	47.6197	-70.1352	05.3	2.0	1162
19960824	02450850	47.4013	-70.3200	11.5	2.0	1168
19960924	06444550	47.5875	-70.1451	21.4	2.0	1171
19961215	18352380	48.2215	-70.1416	00.0	2.0	1176
19970104	12142170	47.6235	-70.1323	09.3	2.0	1180
19970509	04223320	47.6479	-69.8656	14.6	2.0	1189
19970718	22341140	47.6734	-69.9025	09.4	2.0	1192
19970812	17375610	47.6965	-70.1004	00.0	2.0	1197
19970910	01232730	47.5561	-70.3507	04.7	2.0	1202
19971020	16270730	47.6749	-69.9115	13.9	2.0	1204
19971225	05585580	47.5642	-69.9160	13.2	2.0	1217

Date	Time	Latitude	Longitude	Depth(km)	Magnitude(mN)	ID
19971229	09273870	47.7425	-69.9966	10.6	2.0	1219
19980213	20445410	47.4592	-70.1266	11.0	2.0	1223
19980220	22063170	47.4358	-70.1575	21.6	2.0	1226
19980321	23014850	47.5180	-70.2725	07.8	2.0	1230
19980519	13385260	47.5440	-69.9936	11.0	2.0	1235
19980616	09334370	47.4884	-69.9765	13.0	2.0	1237
19980712	03382180	47.5279	-70.0281	14.6	2.0	1239
19980731	21481120	47.3170	-70.4277	07.8	2.0	1240
19980803	02202160	47.6369	-70.1537	12.7	2.0	1242
19981204	08022530	47.4536	-70.1266	16.4	2.0	1250
19991128	08391630	47.4821	-70.3631	06.5	2.0	1263
20000106	18562960	47.3875	-70.2225	12.6	2.0	1265
20000131	02262050	47.4164	-70.4407	04.8	2.0	1269
20000224	02010470	47.5141	-70.0407	12.1	2.0	1272
20000224	02191430	47.5145	-70.0405	12.1	2.0	1273
20000308	14335760	47.6005	-69.9364	12.2	2.0	1274
20000619	03024410	47.5479	-70.0456	14.0	2.0	1281
20001019	20021420	47.6078	-69.9741	09.4	2.0	1290
20001031	19150170	48.2788	-69.8255	00.0	2.0	1293
20010123	18242580	48.0827	-69.7979	00.0	2.0	1299
20010131	05042520	47.1615	-70.3998	07.4	2.0	1300
20010525	15332090	47.6915	-70.2003	00.0	2.0	1310

Date	Time	Latitude	Longitude	Depth(km)	Magnitude(mN)	ID
20010622	03290280	47.3898	-70.1254	16.0	2.0	1314
20011104	11483020	48.4803	-69.9869	18.0	2.0	1328
20011202	08382950	47.5855	-70.0527	24.9	2.0	1331
20020119	13324780	47.4396	-70.0430	14.7	2.0	1336
20020408	16210570	48.4330	-69.3340	18.0	2.0	1344
20020426	15464350	48.4733	-69.3597	00.0	2.0	1346
20020505	08495530	47.4427	-70.4057	14.1	2.0	1349
20020603	18202560	47.7341	-69.9921	15.9	2.0	1352
20020822	04191350	47.5465	-70.2226	17.2	2.0	1357
20021006	01225430	47.5992	-70.1798	08.7	2.0	1360
20021125	12292310	47.3306	-70.1660	12.7	2.0	1366
20021127	09005620	47.5213	-70.0703	12.9	2.0	1367
20021214	01323810	47.3061	-70.4464	06.2	2.0	1369
20030311	21280390	48.2522	-69.6941	00.0	2.0	1374
20030325	22234430	48.2690	-69.6768	00.0	2.0	1375
20030617	10560780	47.7038	-70.0726	11.8	2.0	1380
20030620	11210360	47.6927	-70.0820	12.6	2.0	1382
20030923	06375170	47.7645	-69.6530	23.4	2.0	1391
20031108	10500590	47.6520	-69.9375	16.3	2.0	1393
20040213	02221790	47.4434	-70.3866	06.9	2.0	1401
20040424	21303640	47.4019	-70.3105	16.4	2.0	1404
20040630	12072330	47.5469	-70.1657	18.0	2.0	1412

Date	Time	Latitude	Longitude	Depth(km)	Magnitude(mN)	ID
20040819	21513660	47.4298	-70.3794	12.6	2.0	1416
20040823	16305230	47.5997	-70.3243	00.0	2.0	1417
20041119	20440560	47.5765	-69.9143	13.1	2.0	1424
20041127	12453110	47.6230	-70.0050	27.1	2.0	1425
20041210	21364050	47.6186	-69.9854	08.0	2.0	1426
20050218	23043620	47.6013	-70.2456	17.5	2.0	1432
20050306	15122360	47.7552	-69.7310	15.1	2.0	1435
20050328	23501730	47.5778	-70.1255	18.7	2.0	1437
20050505	02212120	47.7543	-69.7346	14.3	2.0	1439
20050605	09221180	47.6329	-69.9788	27.1	2.0	1442
20050717	20464940	48.0544	-69.1753	00.0	2.0	1443
20050921	18050880	47.8015	-69.8336	22.5	2.0	1447
20051101	23560430	47.5453	-70.1607	18.7	2.0	1450
20051109	05021110	47.4873	-70.1277	08.6	2.0	1452
20051222	20213900	47.5916	-69.9047	14.2	2.0	1455
20060407	02351540	47.5242	-70.2116	14.4	2.0	1459
20060411	19061340	48.1851	-69.7017	00.0	2.0	1461
20060812	00332120	47.4395	-70.1199	13.2	2.0	1469
20061018	19301290	47.4663	-70.4205	00.0	2.0	1473
20070109	17065780	47.3911	-70.2344	12.8	2.0	1483
20070115	08362160	47.5463	-70.1512	22.9	2.0	1484
20070312	03102850	47.8020	-69.7900	22.0	2.0	1486

Date	Time	Latitude	Longitude	Depth(km)	Magnitude(mN)	ID
20070410	08161690	47.5453	-70.3637	07.8	2.0	1488
20070702	03530590	47.8902	-69.8111	13.9	2.0	1493
20070729	18185460	48.2645	-69.6721	18.0	2.0	1496
20071025	01081240	47.5366	-70.3738	03.7	2.0	1499
20080409	01493340	47.1860	-70.4652	18.0	2.0	1506
20080801	18030420	47.4721	-70.4504	00.0	2.0	1514
20081020	15130080	47.6333	-70.4010	10.0	2.0	1516
20081201	21001450	48.1043	-69.0109	00.0	2.0	1519
20090328	03043530	48.4920	-69.1964	18.0	2.0	1523
20090804	20284380	47.6189	-70.3648	00.0	2.0	1528
20090817	06302280	47.6918	-70.0490	10.9	2.0	1529
20090823	07430480	47.5287	-70.3706	04.1	2.0	1531
20090909	18055030	47.7805	-69.8223	21.7	2.0	1533
20100220	16464810	47.7209	-69.9237	25.5	2.0	1543
20100306	19032470	47.4801	-70.1409	14.5	2.0	1547
20100413	19361930	47.7348	-70.2358	00.0	2.0	1551
20100507	21231190	47.4287	-70.3285	19.4	2.0	1554
20100809	18381190	47.6172	-70.1569	11.5	2.0	1559
20101013	02580370	47.6685	-70.2434	09.5	2.0	1569
19880703	03254570	47.6570	-69.9340	10.4	2.1	1010
19880914	05461340	47.5910	-70.0810	21.5	2.1	1015
19890321	22203480	48.2040	-70.4790	01.0	2.1	1027

Date	Time	Latitude	Longitude	Depth(km)	Magnitude(mN)	ID
19890428	11033220	47.3081	-70.4358	08.9	2.1	1028
19890618	10560530	47.4302	-70.0295	08.6	2.1	1030
19890714	00260140	47.4105	-70.3150	12.4	2.1	1031
19890917	14212880	47.7153	-69.7330	16.2	2.1	1036
19900530	02505350	47.5292	-69.9710	11.9	2.1	1052
19900926	19543000	47.4318	-70.3839	04.7	2.1	1056
19901228	06322310	47.3980	-70.2281	13.6	2.1	1064
19910918	17271520	47.3803	-70.0625	24.2	2.1	1070
19920603	03585810	47.4143	-70.3196	10.7	2.1	1088
19920722	22330610	47.5762	-70.2159	11.2	2.1	1090
19920728	10075360	47.4858	-70.0421	01.2	2.1	1092
19921202	20264360	47.8219	-69.9955	06.8	2.1	1096
19930727	05303030	47.4020	-70.1536	18.0	2.1	1109
19940106	15582300	47.4262	-70.1154	10.1	2.1	1117
19950112	09214410	47.5875	-69.9159	18.0	2.1	1129
19950920	02332590	47.4999	-70.4015	05.1	2.1	1143
19951019	03160760	47.5844	-70.0009	09.0	2.1	1146
19951109	20543600	47.8227	-69.9526	18.9	2.1	1149
19960504	16250530	47.6880	-70.2155	00.0	2.1	1157
19960819	17060960	47.3002	-70.2448	06.4	2.1	1167
19970222	01384960	47.6210	-69.9471	09.3	2.1	1185
19970409	02441740	47.3785	-70.4647	11.4	2.1	1186

Date	Time	Latitude	Longitude	Depth(km)	Magnitude(mN)	ID
19970509	14574640	47.5475	-70.0685	20.5	2.1	1190
19970725	12054810	47.5400	-70.3685	00.7	2.1	1193
19971021	17194390	47.4022	-70.4625	10.1	2.1	1205
19971027	15045120	47.5858	-69.9821	09.0	2.1	1206
19971108	11513420	47.4404	-70.0541	14.8	2.1	1211
19971201	22310160	47.7293	-70.0018	14.9	2.1	1215
19980204	18151150	47.6232	-70.1483	11.2	2.1	1221
19980305	03092910	47.5029	-70.3974	02.2	2.1	1229
19980430	15180560	47.5824	-69.9260	12.8	2.1	1231
19980506	07461080	47.6818	-69.9150	11.1	2.1	1232
19980521	15595090	47.6744	-69.9110	08.9	2.1	1236
19980829	18360480	47.4196	-70.4328	05.5	2.1	1244
19990516	00222180	47.6591	-70.2275	07.9	2.1	1254
19990719	21180670	47.5783	-69.8974	15.8	2.1	1256
19990813	05033340	47.4477	-70.0205	11.4	2.1	1259
19991210	02241150	47.4413	-70.1064	07.8	2.1	1264
20000203	02462930	47.4175	-70.4496	05.7	2.1	1270
20000417	06435950	47.4940	-70.0897	14.3	2.1	1276
20001022	15215220	47.4006	-70.4147	04.9	2.1	1291
20010131	13523010	47.5256	-70.1317	14.9	2.1	1301
20010215	07472020	47.5910	-69.9795	09.9	2.1	1302
20010428	07104350	47.4137	-70.2970	13.4	2.1	1305

Date	Time	Latitude	Longitude	Depth(km)	Magnitude(mN)	ID
20010522	00315540	47.6559	-69.9199	08.9	2.1	1307
20010606	05515790	47.5423	-70.1050	10.5	2.1	1311
20010628	18330450	48.4852	-69.3381	18.0	2.1	1315
20010727	23124190	47.6872	-69.8553	14.4	2.1	1318
20010920	22331110	47.4093	-70.0766	21.6	2.1	1321
20011020	01290140	47.4330	-70.3025	15.4	2.1	1324
20011224	02362260	47.4852	-70.1591	15.1	2.1	1333
20020213	22483480	47.4560	-70.0477	12.3	2.1	1338
20020215	11001060	47.5046	-70.0352	11.9	2.1	1339
20020309	00552250	47.6726	-70.1536	10.9	2.1	1341
20020403	18091310	47.4444	-70.4117	07.7	2.1	1342
20020419	21544950	47.4346	-70.1704	09.8	2.1	1345
20020520	18550610	47.6123	-70.2991	17.9	2.1	1351
20020717	00030620	47.7510	-70.1006	10.8	2.1	1355
20021016	14073330	47.4347	-70.3780	06.5	2.1	1361
20021224	09404270	47.5966	-69.9648	09.5	2.1	1372
20030805	18413770	47.4991	-70.0086	16.1	2.1	1385
20030905	03504160	47.3888	-70.2491	09.5	2.1	1389
20030914	22482050	47.7319	-69.7580	20.8	2.1	1390
20031208	04265960	47.4012	-70.3910	05.7	2.1	1397
20040202	07413990	47.5533	-70.2524	13.9	2.1	1399
20040507	14373380	47.4399	-70.0342	10.1	2.1	1406

Date	Time	Latitude	Longitude	Depth(km)	Magnitude(mN)	ID
20041006	18594750	47.3237	-70.1460	07.5	2.1	1419
20041013	17491910	47.5882	-70.1346	25.2	2.1	1420
20041219	00281510	47.4182	-70.4538	11.2	2.1	1428
20050306	08554280	47.7492	-69.7299	13.9	2.1	1434
20050517	07175070	47.7488	-69.7252	14.4	2.1	1440
20050828	04350350	48.1653	-69.4992	18.0	2.1	1445
20051109	08525410	47.3835	-70.1424	14.8	2.1	1453
20060115	09012230	47.3870	-70.2850	15.1	2.1	1456
20060206	11404870	47.4973	-69.9896	06.7	2.1	1458
20060519	00585530	47.8446	-69.9032	23.6	2.1	1462
20060620	06042080	47.8157	-69.9337	22.4	2.1	1466
20061102	03575020	47.5473	-70.1674	17.3	2.1	1476
20061109	22355960	47.8131	-69.7877	22.4	2.1	1477
20061206	00344280	47.7920	-69.9765	19.2	2.1	1480
20070618	20023970	47.5535	-69.8560	17.2	2.1	1492
20070719	23444350	47.4921	-70.1716	08.2	2.1	1495
20070819	06112270	47.2892	-70.3329	10.6	2.1	1497
20071031	12024310	47.3222	-70.4071	06.1	2.1	1500
20080529	01225360	47.6269	-70.1974	13.4	2.1	1509
20081016	17521570	47.6335	-70.2349	00.0	2.1	1515
20090827	19222430	48.3026	-69.3901	18.0	2.1	1532
20090922	22073820	47.7117	-69.9330	25.7	2.1	1535

Date	Time	Latitude	Longitude	Depth(km)	Magnitude(mN)	ID
20100221	03014830	47.4970	-69.9361	13.7	2.1	1544
20100301	00014640	47.5971	-70.1776	10.6	2.1	1546
20100331	02402260	47.5031	-70.1299	11.2	2.1	1549
20100813	00054660	47.4420	-70.2996	13.9	2.1	1561
20100831	02101610	47.4464	-70.3403	14.2	2.1	1563
20100904	12521770	47.3465	-70.4573	11.9	2.1	1564
20100909	04512840	47.3251	-70.4576	12.3	2.1	1566
19880627	01434150	47.3250	-70.3500	04.4	2.2	1009
19880906	00143970	47.5210	-70.1870	12.8	2.2	1014
19891211	04563560	47.8960	-69.9605	10.0	2.2	1040
19900407	13305680	47.5729	-69.9530	12.0	2.2	1049
19901020	03464680	47.3906	-70.1533	09.8	2.2	1058
19901106	02343480	47.4348	-70.3034	11.8	2.2	1061
19910727	02394110	47.5580	-70.0948	16.5	2.2	1069
19920722	23073110	47.5635	-69.9341	13.1	2.2	1091
19930212	09064040	47.7751	-70.1488	08.0	2.2	1098
19930415	09025740	47.6147	-69.8360	21.3	2.2	1101
19950216	17093930	47.4030	-70.2668	14.8	2.2	1130
19960714	07150280	47.4829	-70.0503	13.7	2.2	1163
19960814	21105460	47.3816	-70.1371	13.9	2.2	1166
19960913	23553590	47.5008	-70.2134	12.1	2.2	1169
19960923	05265420	47.6591	-69.8932	14.0	2.2	1170

Date	Time	Latitude	Longitude	Depth(km)	Magnitude(mN)	ID
19960925	08342480	47.8528	-69.7504	22.4	2.2	1173
19961025	09472440	47.4281	-70.3887	04.1	2.2	1174
19961228	17365920	47.8043	-69.8189	17.7	2.2	1178
19970422	23060480	47.6830	-70.1880	05.2	2.2	1188
19970809	18003510	47.4635	-70.0620	17.6	2.2	1196
19970924	17131220	47.7492	-69.9065	22.8	2.2	1203
19971210	08180870	47.4734	-69.9819	11.1	2.2	1216
19980103	09570020	47.4402	-70.1576	10.1	2.2	1220
19980212	03210900	47.4253	-70.4576	03.9	2.2	1222
19980217	03031440	47.3679	-70.4016	07.1	2.2	1225
19980302	01525660	47.4418	-70.3818	09.3	2.2	1228
19980623	17391680	47.7303	-69.9224	24.0	2.2	1238
19980801	16293470	47.5050	-70.2257	23.4	2.2	1241
19980815	07461630	47.6538	-70.1060	15.2	2.2	1243
19980902	06551490	48.1731	-69.2860	18.0	2.2	1245
19980922	21212960	47.7325	-70.0359	05.8	2.2	1247
19981021	18535520	47.4852	-70.0360	15.9	2.2	1249
19990208	20484870	47.4400	-70.1714	22.6	2.2	1252
20000614	20022490	47.3310	-70.1095	19.0	2.2	1279
20000620	20120570	47.4135	-70.0935	08.5	2.2	1282
20001224	00194980	47.3119	-70.4363	20.0	2.2	1298
20010219	03395760	47.8192	-70.1609	25.6	2.2	1303

Date	Time	Latitude	Longitude	Depth(km)	Magnitude(mN)	ID
20010306	02090330	47.4900	-70.0785	07.9	2.2	1304
20010503	20074470	47.4320	-70.1570	11.3	2.2	1306
20010710	12301970	47.4300	-70.0596	18.0	2.2	1317
20011109	10234820	47.5142	-69.9641	07.2	2.2	1329
20020225	06091490	47.5151	-70.1883	17.4	2.2	1340
20020505	01530180	47.9208	-69.7803	23.0	2.2	1348
20021023	08053090	47.5656	-70.0449	10.5	2.2	1362
20021125	03180890	47.7059	-70.0763	12.1	2.2	1365
20030407	19224130	48.2553	-69.7234	00.0	2.2	1376
20030715	13433970	47.4698	-70.0472	06.2	2.2	1383
20030725	04510290	47.7444	-70.0688	11.6	2.2	1384
20030821	07594130	47.6663	-69.8981	09.5	2.2	1387
20031127	09011910	47.6944	-70.0948	05.4	2.2	1395
20040520	03243870	47.4816	-70.0647	06.8	2.2	1407
20040524	22210910	47.8367	-69.8004	21.7	2.2	1409
20040612	12052670	47.5296	-70.0278	14.2	2.2	1411
20040705	14544870	47.5149	-69.9487	09.6	2.2	1414
20040915	01530220	47.5023	-70.0552	12.0	2.2	1418
20041117	21593660	47.6579	-70.1538	04.9	2.2	1422
20050103	10035720	47.2961	-70.4144	06.1	2.2	1429
20050124	10003350	47.5826	-69.9552	10.8	2.2	1430
20051102	19241310	47.5511	-70.2343	12.1	2.2	1451

Date	Time	Latitude	Longitude	Depth(km)	Magnitude(mN)	ID
20061004	08522340	47.4055	-70.3416	18.6	2.2	1472
20061123	19025990	47.4486	-70.3714	05.0	2.2	1478
20070310	23250040	47.8008	-69.7945	21.3	2.2	1485
20070504	12010150	48.1371	-70.0341	18.0	2.2	1490
20080115	03171160	47.7047	-70.1182	08.8	2.2	1503
20080124	14164730	47.4162	-70.1127	09.8	2.2	1504
20080312	01593780	47.5558	-69.9764	15.9	2.2	1505
20080507	04082170	47.6896	-70.2476	00.0	2.2	1508
20090818	15200920	47.3113	-70.4934	06.8	2.2	1530
20091120	02592980	47.8498	-69.7863	26.4	2.2	1537
20100408	01191790	47.5840	-70.0035	07.7	2.2	1550
20100424	11353350	47.5333	-70.0562	15.8	2.2	1552
20100518	22412740	47.5854	-69.8904	16.2	2.2	1555
20100525	14094710	47.5488	-70.1620	19.5	2.2	1556
20100619	23593310	47.7160	-69.7747	27.5	2.2	1557
19880315	08043570	47.5290	-70.0050	09.4	2.3	1004
19880812	20130440	47.5970	-70.1980	04.0	2.3	1013
19890317	22374340	48.2470	-70.3790	01.0	2.3	1025
19890525	18562170	47.5807	-69.8959	16.3	2.3	1029
19900307	16090900	47.6730	-70.1880	00.0	2.3	1045
19900331	06053420	47.6215	-70.1587	09.4	2.3	1048
19910930	18291740	47.4943	-70.3659	06.7	2.3	1072

Date	Time	Latitude	Longitude	Depth(km)	Magnitude(mN)	ID
19911205	08502620	47.7147	-70.0494	11.0	2.3	1076
19920124	01370350	47.5270	-70.0943	07.9	2.3	1079
19920505	00411920	47.5918	-69.9505	11.3	2.3	1087
19920616	20114670	47.4074	-70.3404	08.0	2.3	1089
19930223	09515120	47.4914	-69.9860	11.6	2.3	1099
19930602	22000180	47.4533	-70.1746	22.4	2.3	1105
19930705	18325430	47.4401	-70.1897	06.2	2.3	1107
19930818	15032670	47.4557	-70.1039	12.2	2.3	1111
19930904	08211230	47.4582	-70.1726	14.3	2.3	1113
19950817	01525740	47.4198	-70.4041	12.0	2.3	1140
19950823	12301880	47.4293	-70.3307	11.7	2.3	1141
19950924	14270640	47.6443	-69.9524	08.0	2.3	1144
19960329	15104070	47.9606	-69.4713	00.0	2.3	1154
19960726	14384510	47.6097	-69.9468	10.4	2.3	1165
19961028	02453920	47.5536	-70.0414	11.6	2.3	1175
19961222	00303200	47.5059	-70.0637	10.8	2.3	1177
19970111	07504920	47.5361	-70.0450	11.5	2.3	1182
19970218	16544280	48.2189	-70.2430	00.0	2.3	1184
19971228	20395770	47.7938	-69.9336	27.6	2.3	1218
19980515	22173650	47.6405	-70.0638	23.8	2.3	1233
19990812	03092870	47.5691	-70.0042	15.4	2.3	1258
20000314	00372120	47.6214	-69.8861	14.8	2.3	1275

Date	Time	Latitude	Longitude	Depth(km)	Magnitude(mN)	ID
20000429	01510820	47.4839	-70.1415	21.8	2.3	1278
20001010	22201490	47.3835	-70.4480	12.8	2.3	1288
20001026	09245230	47.2841	-70.2181	08.5	2.3	1292
20001103	17210320	47.4218	-70.0589	11.6	2.3	1294
20001212	13482450	47.5741	-70.1987	16.0	2.3	1297
20010705	10325540	47.2414	-70.3386	08.6	2.3	1316
20010819	17200220	47.4332	-70.1559	12.1	2.3	1319
20011025	08115970	47.3390	-70.1977	23.6	2.3	1325
20011026	05083050	47.3624	-70.2330	12.9	2.3	1326
20020115	04314980	47.5501	-70.0310	08.5	2.3	1334
20020428	02020550	47.4355	-70.4277	04.6	2.3	1347
20021005	09343540	47.4531	-70.3904	21.9	2.3	1359
20021122	21190310	47.5570	-70.2922	08.1	2.3	1363
20031205	04592070	47.4320	-70.1251	08.6	2.3	1396
20040422	10030350	47.3208	-70.3049	13.5	2.3	1403
20040809	16472240	47.7184	-69.8718	17.2	2.3	1415
20050311	00362340	47.7622	-69.7318	12.7	2.3	1436
20050806	01175860	47.5634	-70.0563	11.2	2.3	1444
20060915	04420880	47.4597	-70.0337	10.6	2.3	1471
20061126	19193020	47.5923	-69.9363	11.7	2.3	1479
20070703	03283330	47.5799	-70.2433	07.1	2.3	1494
20080107	01385240	47.3218	-70.3228	11.4	2.3	1502

Date	Time	Latitude	Longitude	Depth(km)	Magnitude(mN)	ID
20080725	01403740	47.5479	-69.9221	14.2	2.3	1513
20090606	17511380	47.5841	-70.2781	10.8	2.3	1526
20090914	22092240	47.6039	-70.1044	24.4	2.3	1534
20091201	01444190	47.6507	-69.8735	14.4	2.3	1539
20091205	23312270	47.5462	-70.0306	13.4	2.3	1540
20100227	16364780	47.6031	-70.1527	14.4	2.3	1545
20100827	09435480	47.6705	-69.9023	06.5	2.3	1562
19880124	01075670	47.4410	-70.4540	10.2	2.4	1001
19880715	15572780	47.2500	-70.0770	18.0	2.4	1011
19880804	22334970	47.4810	-70.1050	12.4	2.4	1012
19900313	18494050	47.5338	-70.1374	15.5	2.4	1046
19901230	16335510	47.6717	-70.0201	25.3	2.4	1065
19911217	02091580	47.5729	-70.2310	15.6	2.4	1078
19920807	03323840	47.5794	-70.2047	09.8	2.4	1093
19930518	00174170	47.5432	-70.0329	07.6	2.4	1104
19940316	07230570	47.4398	-70.0436	09.8	2.4	1119
19940602	14453710	47.7178	-69.9481	25.4	2.4	1121
19940621	07501190	47.4402	-70.0499	08.0	2.4	1122
19950112	03240810	47.6066	-69.9523	11.8	2.4	1128
19950304	10522340	47.3039	-70.4349	08.5	2.4	1132
19951104	09325770	47.6025	-69.9859	17.8	2.4	1148
19960404	15130200	47.5732	-70.1014	18.9	2.4	1155

Date	Time	Latitude	Longitude	Depth(km)	Magnitude(mN)	ID
19970422	11004500	47.6065	-70.2164	15.1	2.4	1187
19970730	15561310	47.5829	-70.2053	06.2	2.4	1194
19970806	01322910	47.5838	-69.9472	14.9	2.4	1195
19970903	23061250	47.5344	-69.8869	13.0	2.4	1200
19971031	15412060	47.5372	-70.0386	07.8	2.4	1210
19971118	22454650	47.4238	-70.4323	05.5	2.4	1213
19971128	10563530	47.6754	-69.9149	09.1	2.4	1214
19980519	01163390	47.3472	-70.3820	06.8	2.4	1234
19980904	15420390	47.5479	-70.2292	14.1	2.4	1246
19981225	16464940	47.3504	-70.3061	09.7	2.4	1251
20000417	22301590	47.3413	-70.2008	15.8	2.4	1277
20000621	12164440	47.6470	-69.9100	13.1	2.4	1283
20001201	02501610	47.5236	-70.2134	13.3	2.4	1295
20001204	06445410	47.3995	-70.1735	10.3	2.4	1296
20011026	12574180	47.3915	-70.1118	17.5	2.4	1327
20011205	18482720	47.5500	-70.2535	09.2	2.4	1332
20020404	22373460	47.2120	-70.4038	11.4	2.4	1343
20021004	15342590	47.5607	-70.2641	00.0	2.4	1358
20021124	16242340	47.5078	-69.9603	12.3	2.4	1364
20021221	08301570	47.5108	-70.2059	13.5	2.4	1371
20030612	13074060	47.8078	-69.7488	24.3	2.4	1378
20030825	08533050	47.6258	-69.9429	15.5	2.4	1388

Date	Time	Latitude	Longitude	Depth(km)	Magnitude(mN)	ID
20031120	19544730	47.4676	-70.1098	11.0	2.4	1394
20040204	15015320	47.6638	-70.1168	06.5	2.4	1400
20040425	20411720	47.6231	-70.1768	12.5	2.4	1405
20041105	07113460	47.3839	-70.4223	05.1	2.4	1421
20041215	19172640	47.5960	-70.0287	26.6	2.4	1427
20050412	14482490	47.7163	-70.0701	09.0	2.4	1438
20050601	18105620	47.5748	-70.3334	09.9	2.4	1441
20051003	07214490	47.5643	-70.0141	14.7	2.4	1448
20060609	14513220	47.5097	-70.1897	18.1	2.4	1464
20060614	10425550	47.7961	-69.9505	19.8	2.4	1465
20061101	09293610	47.6121	-70.1721	13.9	2.4	1475
20070609	09274840	47.5764	-70.3223	11.0	2.4	1491
20080703	11045710	47.4177	-70.3401	10.9	2.4	1511
20080704	02504260	47.7573	-69.7618	20.6	2.4	1512
20090312	22203780	47.4158	-70.3296	12.2	2.4	1521
20090929	23462750	47.7181	-70.2600	00.0	2.4	1536
20100723	15281650	47.5471	-70.2526	13.1	2.4	1558
20100930	03455360	47.4941	-70.1368	07.7	2.4	1567
19880610	18451370	47.5900	-69.9410	12.7	2.5	1007
19881216	18554670	48.2880	-69.6000	18.0	2.5	1017
19890801	23421910	47.7104	-69.8891	12.3	2.5	1032
19891229	15325760	47.4979	-70.1446	06.0	2.5	1042

Date	Time	Latitude	Longitude	Depth(km)	Magnitude(mN)	ID
19900716	11465390	47.6171	-69.9705	07.7	2.5	1053
19900921	09114270	47.5510	-70.2648	13.4	2.5	1054
19910219	07170210	47.4633	-69.9986	11.6	2.5	1066
19930718	12331580	47.6019	-70.2282	04.8	2.5	1108
19940624	07252370	47.4437	-70.3182	12.1	2.5	1123
19950704	11410390	47.6003	-70.0981	26.6	2.5	1137
19950812	17425580	47.6680	-69.9035	10.8	2.5	1139
19950930	00011950	47.4219	-70.2684	17.4	2.5	1145
19970101	17141520	47.4411	-70.1105	23.8	2.5	1179
19970903	15522740	47.4750	-70.0563	08.8	2.5	1199
19970909	18204980	47.3667	-70.4060	07.9	2.5	1201
19971028	16540310	47.6782	-69.9104	10.5	2.5	1209
19980225	17060270	48.2591	-69.3985	18.0	2.5	1227
19990418	20210090	47.4364	-70.4685	09.2	2.5	1253
20000209	23422290	47.4787	-69.9758	13.1	2.5	1271
20000703	11014340	47.4310	-70.1579	11.6	2.5	1284
20000816	11522610	47.7884	-69.9283	15.7	2.5	1285
20001012	14161170	47.5907	-69.9976	11.7	2.5	1289
20010619	05215480	47.6938	-70.1046	11.3	2.5	1313
20010908	05312170	47.7921	-69.8611	23.0	2.5	1320
20010921	04430440	47.6885	-70.0970	04.8	2.5	1322
20011111	13222270	47.8625	-69.9275	25.9	2.5	1330

Date	Time	Latitude	Longitude	Depth(km)	Magnitude(mN)	ID
20020131	20515480	47.3505	-70.3977	11.9	2.5	1337
20030618	18545660	47.4513	-70.0745	09.6	2.5	1381
20031219	12401720	47.4732	-70.1334	12.9	2.5	1398
20050203	10121940	47.5727	-70.2261	06.5	2.5	1431
20050831	23374950	47.4592	-70.1319	14.8	2.5	1446
20051114	04551610	47.4026	-70.1937	06.7	2.5	1454
20060204	04394810	47.4928	-69.9804	07.2	2.5	1457
20060721	16174740	47.3466	-70.3411	24.3	2.5	1467
20060817	13293050	47.5131	-70.2994	10.8	2.5	1470
20061229	06001540	47.3556	-69.9337	17.0	2.5	1482
20080426	08161730	47.8090	-69.8092	23.0	2.5	1507
20090104	19162190	48.3965	-69.3809	18.0	2.5	1520
20100220	04411730	47.4357	-70.3905	06.3	2.5	1542
20100811	13032190	47.4182	-70.3071	12.9	2.5	1560
19890224	22531050	47.3629	-70.4486	12.8	2.6	1019
19890831	19442050	47.6131	-70.2855	22.4	2.6	1034
19891208	17203440	47.7009	-70.0644	10.4	2.6	1039
19910919	11065310	47.5384	-69.9324	13.6	2.6	1071
19930605	04494090	47.4931	-70.1126	11.0	2.6	1106
19950918	16094730	47.6678	-69.9033	10.6	2.6	1142
19960430	12502330	47.6200	-70.3115	21.5	2.6	1156
19971111	20143210	48.1964	-70.2943	00.0	2.6	1212

Date	Time	Latitude	Longitude	Depth(km)	Magnitude(mN)	ID
19981021	07445170	47.5583	-70.2836	09.8	2.6	1248
19990726	17351890	47.4798	-70.1192	20.5	2.6	1257
20000110	16550080	47.6897	-69.8787	14.6	2.6	1266
20020119	01180510	47.4787	-70.1066	22.9	2.6	1335
20021211	03180850	47.3078	-70.4414	06.4	2.6	1368
20021218	02321220	47.6009	-69.9749	15.8	2.6	1370
20040704	05100410	47.2271	-70.3229	14.2	2.6	1413
20041118	16475120	47.6468	-70.2212	06.7	2.6	1423
20051024	21104350	47.5417	-70.2676	13.2	2.6	1449
20070330	11101370	47.6729	-70.2239	11.0	2.6	1487
20070501	11291510	48.3636	-69.6213	18.0	2.6	1489
20090324	01365620	47.7105	-70.2760	06.1	2.6	1522
20090428	13071310	47.7864	-69.8872	19.4	2.6	1525
20091128	11413170	47.4208	-70.3979	18.5	2.6	1538
20100122	21270940	47.1848	-70.2484	00.0	2.6	1541
19890830	08254860	47.6597	-70.0545	20.8	2.7	1033
19911124	01175250	47.6145	-70.2191	13.1	2.7	1074
19931202	09031790	47.4552	-70.0428	07.7	2.7	1115
19950615	15591720	47.7155	-69.9275	25.4	2.7	1135
19960117	00422380	47.4807	-70.1452	11.7	2.7	1152
19990918	16095090	47.5150	-70.0360	12.2	2.7	1260
20000127	13210390	48.3243	-69.2523	18.0	2.7	1268

Date	Time	Latitude	Longitude	Depth(km)	Magnitude(mN)	ID
20000921	20263820	47.4898	-69.9776	07.4	2.7	1286
20020620	06100840	47.4447	-70.0493	07.3	2.7	1354
20030609	19325510	47.5828	-69.9249	17.1	2.7	1377
20060608	09375990	47.5899	-69.9838	07.9	2.7	1463
20061225	18131420	47.5165	-70.0174	14.8	2.7	1481
20101018	01582150	47.7054	-69.9633	24.4	2.7	1570
19890312	07203960	47.4482	-70.1176	19.7	2.8	1024
19891218	14553560	47.3866	-70.1543	18.2	2.8	1041
19901018	06032840	47.4817	-70.0868	15.2	2.8	1057
19911125	17085910	47.4024	-70.1770	10.1	2.8	1075
19930423	00075010	47.6312	-69.8236	12.0	2.8	1102
19940711	09354110	47.5620	-70.0513	04.9	2.8	1124
19950518	15444970	47.5023	-70.0445	14.6	2.8	1134
19960226	02010860	47.6987	-70.1064	10.3	2.8	1153
19970618	21305930	47.6880	-70.1935	05.4	2.8	1191
19990609	01350160	47.7023	-69.8932	11.2	2.8	1255
19991028	01520890	47.7101	-69.8636	15.3	2.8	1262
20000115	04505220	47.4459	-70.2334	24.0	2.8	1267
20010610	15593290	47.2863	-70.2094	16.8	2.8	1312
20020813	18315960	48.4222	-69.2934	18.0	2.8	1356
20060808	03094440	47.6902	-70.0061	19.4	2.8	1468
20080614	07103430	47.8071	-69.7331	21.9	2.8	1510

Date	Time	Latitude	Longitude	Depth(km)	Magnitude(mN)	ID
20081110	06125730	47.4350	-70.4100	05.3	2.8	1517
20100904	22135360	47.4704	-70.3856	05.4	2.8	1565
19890913	14552360	47.5700	-70.0395	14.8	2.9	1035
19911030	23252910	47.7831	-69.9574	17.2	2.9	1073
19920404	12302850	47.4325	-70.1733	18.9	2.9	1084
19930424	06452420	47.6675	-69.9036	09.1	2.9	1103
19951226	14511010	47.3996	-70.1822	12.8	2.9	1150
20011003	05292080	47.4004	-70.4792	09.9	2.9	1323
20030817	06000350	47.5551	-70.0436	08.5	2.9	1386
20090618	02475280	47.5439	-69.8907	15.8	2.9	1527
19900423	00280470	47.4141	-70.1788	08.2	3.0	1051
19910703	09264230	47.5292	-70.1464	18.4	3.0	1068
19941201	13024710	47.4374	-70.3137	10.8	3.0	1127
19980216	05403580	47.3575	-70.3856	25.3	3.0	1224
19991002	09453660	47.4171	-70.1182	08.7	3.0	1261
20000927	12420190	47.4734	-70.0372	08.1	3.0	1287
20040524	12184340	47.6372	-70.1850	13.6	3.0	1408
20061031	02414130	47.6152	-70.1803	14.4	3.0	1474
20101007	23105330	47.4076	-70.3302	14.0	3.0	1568
19880124	04333520	47.4400	-70.4560	10.5	3.1	1002
19880313	16243990	47.4450	-70.3760	06.8	3.1	1003
19900421	01230410	47.5532	-70.0699	09.6	3.1	1050

Date	Time	Latitude	Longitude	Depth(km)	Magnitude(mN)	ID
19901026	09135150	47.5692	-69.9848	10.9	3.1	1060
19930304	22022180	47.5145	-70.3617	04.3	3.1	1100
19930807	21253120	47.6659	-69.8856	05.5	3.1	1110
19960512	11532190	47.5161	-70.0281	14.8	3.1	1159
19960607	09414280	47.5299	-69.9417	13.3	3.1	1161
19960924	23410290	47.5477	-70.2411	12.5	3.1	1172
19970114	04473240	47.6567	-69.8766	14.6	3.1	1183
20010522	00364730	47.6532	-69.9173	10.9	3.1	1309
20020514	07263960	47.6551	-69.9670	14.1	3.1	1350
20020612	17141820	47.5098	-70.0180	07.8	3.1	1353
20031011	00100240	47.5345	-69.8575	23.2	3.1	1392
20100310	06411890	47.6853	-70.1033	10.4	3.1	1548
20100505	22191810	47.5762	-70.0884	19.1	3.1	1553
19891013	14044280	47.3926	-70.1330	22.7	3.2	1037
19900313	19103930	47.5338	-70.1366	15.3	3.2	1047
19900921	19330140	47.5777	-70.2374	04.1	3.2	1055
19920501	00375140	47.4463	-70.4069	02.7	3.2	1086
19970110	19272750	47.5094	-70.1965	17.0	3.2	1181
19971028	11454860	47.6680	-69.9056	07.6	3.2	1208
20040410	05231870	47.8255	-69.8138	27.5	3.2	1402
20090412	06482610	47.5206	-70.0564	12.6	3.2	1524
19901021	13384320	47.3975	-70.3640	15.8	3.3	1059

Date	Time	Latitude	Longitude	Depth(km)	Magnitude(mN)	ID
19901218	07104620	47.2629	-70.3358	09.3	3.3	1063
19920310	05453260	47.7167	-69.8575	09.9	3.3	1081
20030228	09404720	47.5031	-70.0257	08.6	3.3	1373
20040529	21211610	47.4407	-70.1689	06.5	3.3	1410
20070927	11310850	47.4114	-70.3712	14.5	3.3	1498
19891122	23025170	47.4558	-70.3430	07.6	3.4	1038
19901106	11301070	47.3945	-70.1506	14.2	3.4	1062
19960714	18464920	47.6938	-69.9927	07.3	3.4	1164
20080103	09375550	47.3821	-70.3120	13.5	3.4	1501
19931201	12471580	47.4670	-70.1584	18.0	3.5	1114
20010522	00332910	47.6539	-69.9198	11.4	3.5	1308
19880102	09251730	47.4180	-70.4310	10.8	3.6	1000
19900303	02060330	47.8558	-69.9765	20.8	3.6	1043
19970820	09120440	47.5365	-70.2921	07.5	3.7	1198
20000615	09255410	47.6731	-69.8032	11.4	3.7	1280
19931230	23014760	47.4532	-70.3624	06.2	3.8	1116
20030613	11344020	47.7034	-70.0871	11.1	4.1	1379
20060407	08314150	47.3792	-70.4625	24.5	4.1	1460
20081115	10525430	47.7394	-69.7350	13.3	4.2	1518
19890309	09413220	47.7170	-69.8567	10.5	4.3	1022
19911208	03003090	47.7796	-69.8640	23.2	4.3	1077
19940925	00532870	47.7667	-69.9630	17.0	4.3	1126

Date	Time	Latitude	Longitude	Depth(km)	Magnitude(mN)	ID
19890311	08315220	47.7191	-69.8744	10.3	4.4	1023
19971028	11441860	47.6718	-69.9051	11.3	4.7	1207
20050306	06174970	47.7528	-69.7321	13.3	5.4	1433

APPENDIX B
Appendix B List of all Clusters

Number of clusters is 11 for min. number of links set to 3

Cluster 1: 434 events

1062 1236 1487 1524 1511 1481 1259 1492 1495 1494 1255 1007 1483 1499 1549 1262

1498 1243 1566 1530 1531 1257 1556 1545 1526 1513 1484 1505 1501 1246 1564 1266

1004 1544 1538 1542 1529 1009 1024 1001 1002 1258 1028 1568 1276 1534 1055 1560

1547 1013 1527 1014 1254 1517 1491 1488 1565 1248 1016 1554 1037 1503 1071 1038

1008 1039 1041 1019 1042 1548 1540 1022 1081 1044 1539 1023 1085 1046 1047 1088

1048 1090 1049 1005 1050 1095 1051 1099 1100 1569 1103 1053 1029 1106 1107 1108

1030 1561 1006 1558 1113 1031 1059 1552 1060 1032 1061 1555 1252 1122 1504 1500

1546 1250 1035 1567 1066 1249 1131 1067 1133 1068 1069 1136 1137 1070 1139 1140

1141 1072 1143 1144 1145 1074 1147 1075 1076 1150 1151 1152 1078 1155 1550 1079

1080 1159 1160 1161 1082 1163 1165 1166 1084 1168 1169 1170 1171 1086 1087 1174

1175 1177 1089 1179 1180 1181 1182 1091 1026 1010 1187 1188 1189 1190 1191 1097

1193 1194 1195 1196 1102 1052 1199 1200 1104 1202 1054 1105 1205 1206 1207 1208

1209 1210 1211 1056 1003 1562 1057 1217 1112 1559 1221 1222 1223 1058 1225 1115

1228 1563 1117 1231 1232 1118 1119 1235 1120 1237 1521 1239 1240 1242 1123 1244

1124 1247 1125 1034 1064 1553 1127 1253 1015 1128 1256 1129 1130 1509 1260 1261

1132 1263 1264 1265 1134 1267 1269 1270 1271 1272 1273 1274 1275 1138 1277 1278

1280 1281 1282 1283 1284 1142 1286 1287 1288 1289 1290 1291 1146 1294 1295 1296

1297 1148 1301 1302 1304 1305 1306 1307 1308 1309 1153 1311 1313 1314 1156 1317 1318 1319 1158 1321 1322 1323 1324 1326 1327 1329 1162 1331 1332 1333 1334 1335 1336 1337 1338 1339 1340 1341 1342 1345 1347 1349 1350 1351 1172 1353 1354 1355 1357 1358 1359 1360 1361 1362 1363 1364 1365 1366 1367 1368 1369 1370 1371 1372 1373 1183 1185 1093 1377 1186 1379 1380 1381 1382 1383 1384 1385 1386 1387 1388 1389 1192 1393 1394 1395 1396 1397 1398 1399 1400 1401 1197 1198 1404 1405 1406 1407 1408 1201 1410 1411 1412 1414 1415 1416 1204 1418 1420 1421 1422 1423 1424 1425 1426 1427 1428 1429 1430 1431 1432 1213 1109 1214 1110 1437 1438 1216 1111 1441 1442 1444 1446 1220 1448 1449 1450 1451 1452 1453 1454 1455 1456 1457 1458 1459 1226 1463 1464 1229 1116 1230 1469 1470 1471 1472 1473 1474 1475 1476 1234 1478 1479

Cluster 2: 36 events

1570 1135 1543 1537 1535 1533 1525 1126 1510 1507 1486 1485 1238 1121 1480 1477 1466 1465 1462 1447 1219 1215 1203 1409 1402 1378 1178 1173 1352 1330 1320 1043 1077 1149 1073 1285

Cluster 3: 8 events

1036 1518 1440 1439 1436 1435 1434 1433

Cluster 4: 7 events

1551 1508 1094 1536 1045 1157 1310

Cluster 5: 7 events

1251 1502 1497 1063 1403 1083 1316

Cluster 6: 3 events

1065 1033 1233

Cluster 7: 2 events

1528 1417

Cluster 8: 2 events

1512 1390

Cluster 9: 2 events

1467 1224

Cluster 10: 2 events

1300 1018

Cluster 11: 2 events

1167 1292